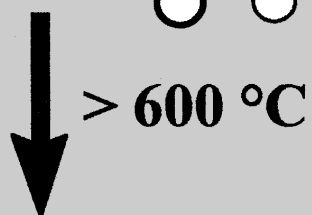
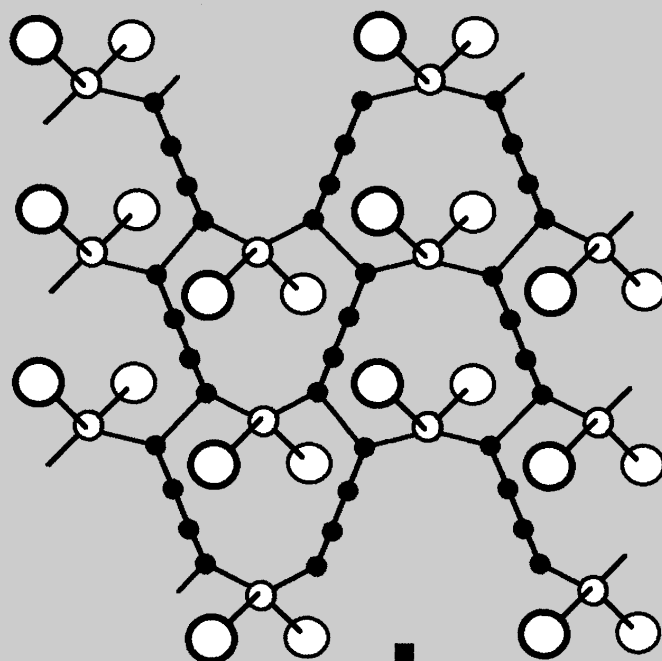
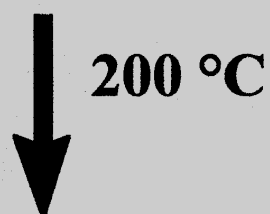
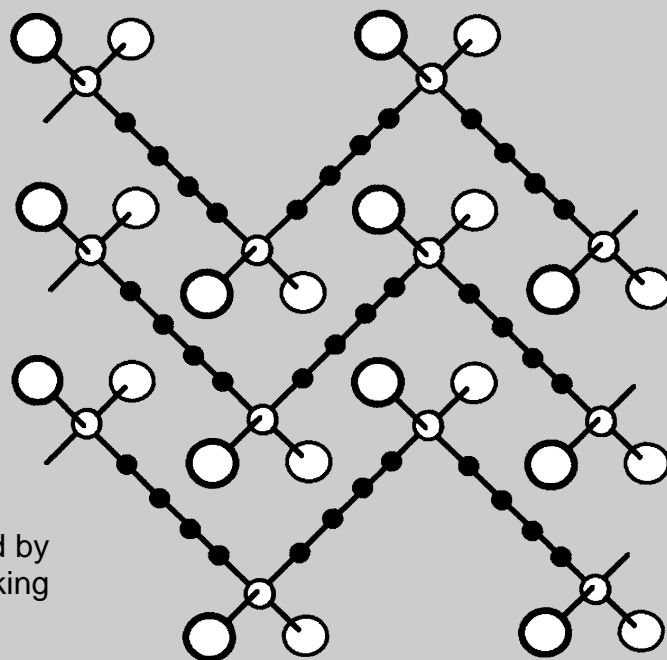


SiC formation in a
carbon matrix obtained by
bisacetylenic cross-linking



Ceramics and Nanostructures from Molecular Precursors

Robert J. P. Corriu*

The elaboration of solids from the molecular scale by a kinetically controlled methodology is one of the main challenges of molecular chemistry. In the long term, this should permit the design of solids with desired properties. Here, some examples are given which show a few methods that have been used for the preparation of solids from molecular precursors. The one-pot synthesis of rheologically controlled SiC is

described. Access to a new kind of ceramic is obtained by the same methodology using molecular precursors. Mixed ceramics with interpenetrating networks are not accessible by the chemical thermodynamic route. The chemistry of hybrid materials obtained from molecular precursors through inorganic polymerization is presented. This class of materials offers wide perspectives because of 1) the large

possibilities opened by the organic unit, 2) the kinetic control, which permits any kind of texture for the solid, and 3) the aptitude of these solids to become nanostructured.

Keywords: ceramics • materials science • nanostructures • polymers • silicon

1. Introduction

The evolution of chemistry is now more and more controlled by developments in life sciences and in material sciences. All the classical divisions of chemistry are concerned with these two highly demanding trends, and little by little a change can be observed corresponding to an ever closer interaction between the different subdisciplines of chemistry, a change necessitated by a variety of new research objectives. For example, both solid-state chemistry and polymer chemistry have borrowed from, and even created, methods belonging to the realm of physical chemistry. The development of modern catalysis involves the chemistry and physical chemistry of surfaces, as well as organometallic coordination chemistry and the design of solid catalyst supports. Molecular chemistry, which is the fruit of cross-fertilization between organic and main group element chemistry, will grow over the next few years to become the chemistry of the elaboration of solids.

The use of molecular chemistry was very successful in opening new routes for chemical synthesis and in explaining the microscopic approach to chemical reactivity. Many synthetic tools were developed with some great successes, including the step-by-step construction of very complicated

natural architectures (e.g. vitamine B₁₂^[1] and palytoxine^[2]). Molecular chemistry was also successfully applied for elaborating sophisticated, purely inorganic molecules (i.e., ladder polymers,^[3] polysilahedranes,^[4] and complicated phosphorus rings^[5]) and for controlling the elaboration of clusters,^[6] polyoxometallic anions,^[7] and dendrimers.^[8]

In material science and solid-state chemistry, solids are classically prepared by thermodynamic routes. In contrast, both organic and inorganic molecular synthetic chemistry are based on the kinetic control of reactions. This molecular approach to synthesis is a multistep approach that implies a good knowledge of reaction mechanisms and product distribution. Until now, this method was not used extensively in materials synthesis. However, polymer elaboration, which is strongly connected to the molecular approach in that it requires a very precise knowledge of reactions mechanism, must be pointed out as the exception.

The elaboration of ceramic fibers and chemical vapor deposition from organometallic compounds (OMCVD) are the first approaches to preparing materials from molecular precursors. The pioneering work of Verbeeck and Winter^[9] and Yajima et al.^[10] were certainly the first attempts for building up a material starting from a single molecule or compound. They succeeded in preparing films and fibers of highly thermomechanically resistant materials (silicon carbides and oxycarbides as well as silicon nitrides and oxynitrides).

Many interesting possibilities were created by the development of "chimie douce" processes^[11, 12] and sol-gel polymerization, which is particularly well adapted for bridging solid-

[*] Prof. R. J. P. Corriu

Laboratoire de Chimie Moléculaire
et Organization du solide – UMR 5637
CC 007 – Université Montpellier II
Place E. Bataillon, 34095 Montpellier Cedex 5 (France)
Fax: (+33)4-67-14-38-52

state and molecular chemistry.^[13] Thus, nowadays one of the main challenges for molecular chemistry is the control of properties by elaboration of solid materials beginning at the molecular scale. The most ambitious aim is to create chemistry that permits control of the organization of properties in the material using a step-by-step synthesis.

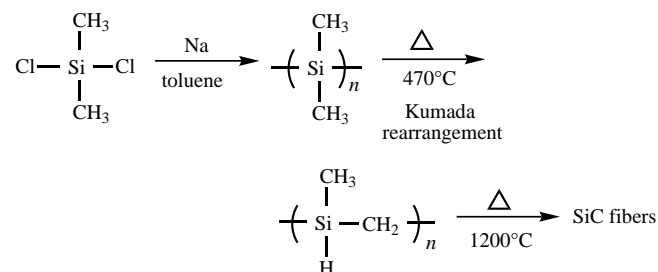
This review describes the main results obtained during the last decade in our attempts to elaborate materials and nanostructures using molecular precursors. These results are given as an example, as other results have been published.^[22]

2. SiC Films and Matrixes via a Rheologically Controlled Preceramic Polymer

2.1. SiC Fibers obtained by the Yajima Process

SiC fibers have been obtained by the discovery of a step-by-step process beginning with $(\text{CH}_3)_2\text{SiCl}_2$ ^[9, 10] (Scheme 1).

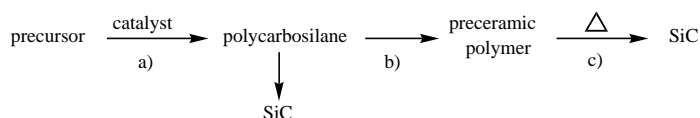
The polydimethylsilane is rearranged into a polycarbosilane by thermal treatment. This preceramic polymer is exposed to high temperature, leading to a polymer whose rheology permits processing (after heating) of silicon oxy-carbide fibers. This process is a great chemical success since it is the only way to obtain, as a fiber, a material that offers high thermomechanical properties (Nicalon fibers are highly resistant until 1200 °C). However, if we consider this process from the chemical point of view, it is a stoichiometric process involving the use of sodium or potassium. It is also possible to consider another route that permits one to synthesize the polycarbosilane by a catalytic reaction.



Scheme 1. The Yajima process for obtaining SiC fibers.

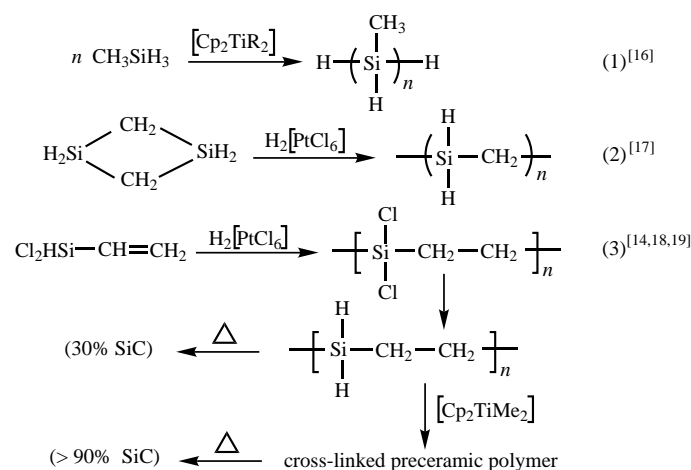
2.2. Catalytic Access to Polycarbosilanes

A general access to SiC using a catalytic procedure has been described (Scheme 2). The polycarbosilane is elaborated by a catalytic reaction in the first step (a). However, the direct pyrolysis of this polymer can lead to a low yield of SiC.^[14] Cross-linking (step b) is necessary for preparing a preceramic polymer that can be transformed into SiC in good yield and with a controlled morphology, which then allows the formation of films or fibers (step c).^[15]



Scheme 2. The principle for catalytic access to SiC.

Three ways have been developed based on hydrosilanes (Scheme 3). For systems represented by reactions (1) and (2), the cross-linking step is not separated from the pyrolysis. In the case of reaction (1) the polymerization leads to a partially cross-linked polymer which can be transformed into SiC with



Scheme 3. Catalytic routes to SiC.



Robert Corriu, born in 1934 in Port-Vendres, France, obtained his *Docteur es Sciences Physiques* in 1961 from the *Université de Montpellier*. He became Assistant Professor at the *Université de Perpignan* in 1963, Associate Professor at the *Université de Poitiers* in 1964, and Professor at the *Université de Montpellier* in 1969. His research interests in organometallic chemistry have been focused on organosilicon, organogermanium, and organophosphorus compounds, transition metal complexes, and hypercoordinated silicon and phosphorus compounds. More recently, he has concentrated his research efforts on the elaboration of solids from molecular precursors. His main interest is now connected with hybrid organic-inorganic materials and molecular chemistry permitting organization of solids. He has obtained awards from the French Chemical Society (*Prix Sue* in 1969 and *Prix Lebel* in 1985), the CNRS (silver medal in 1982), and the American Chemical Society (*Kipping Award* in 1984). He was elected to the French Academy of Sciences in 1991 and the Polish Academy in 1997. He obtained the Alexander von Humboldt Research Award in 1992, the Max Planck Research Award in 1993, and the Wacker Silicon Award in 1998.

77% conversion. The results reported in reaction (2) correspond to the formation of SiC in 96% yield. Cross-linking occurs during the mineralization step.

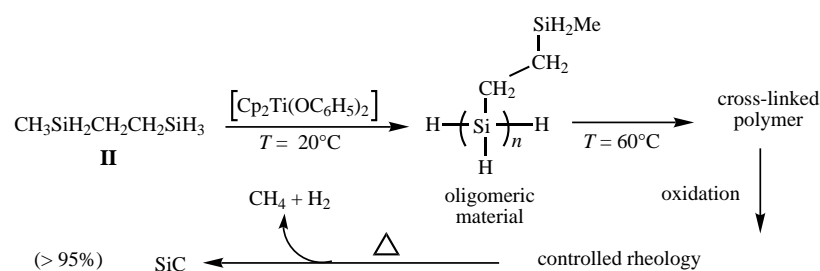
In contrast, in reaction (3), we observed a very great difference in the yield of SiC when the pyrolysis is performed with or without the cross-linking step.^[20] The polymer (SiH₂-CH₂CH₂)_n has been characterized as a soluble linear polymer corresponding to a degree of polymerization ranging from 20 to 95, depending on the experimental conditions, and containing SiH₃ and SiH₂CH=CH₂ chain ends. After pyrolysis, the ceramic yield is low (about 30%), and it is still lower when the vinylic end groups are not present.^[20] As expected the linear polymers which do not cross-link^[18-20] decompose on pyrolysis without giving ceramic residue in acceptable yields. However, after cross-linking with Harrod's catalyst,^[16] it is possible to obtain pure SiC in good yields.^[19]

2.3. Preceramic Polymers with Controlled Rheology

We have succeeded in obtaining a preceramic polymer with a controlled rheology by a one-pot procedure. This process makes use of very simple silaalkanes: 1,4-disilabutane (**I**), 1,4-disilapentane (**II**), and 2,5-disilahexane (**III**).^[19-21]

These precursors were cross-linked separately using Harrod-type catalysts [Cp₂TiR₂] (R = Me, OC₆H₅, etc.). The first step, performed at low temperatures, leads to an oligomeric material. Increasing the temperature from room temperature to 60 °C induces an increase in molecular weight and some cross-linking. To control the rheology of the preceramic polymer, it is possible to poison the catalyst by very brief contact with air. This oxidation is reversible since the medium is highly reductive owing to the great number of Si-H bonds. This method permits control of the cross-linking, making it possible to obtain rheologically controllable material (films or matrixes) before pyrolytic conversion into ceramics. Interestingly, all the precursors provide pure SiC in good yields without excess of C nor Si.^[21] Scheme 4 shows results obtained for 1,4-disilapentane.

This summary of the preparation of ceramics having high thermomechanical performance, such as SiC, illustrates the potential of molecular chemistry. This step-by-step approach is the only method that provides access to ceramic films or fibers with exceptional thermomechanical properties such as SiC or Si₃N₄ and the corresponding silicon oxycarbides and silicon oxycarbonitrides. Since this work was completed, new precursors have been obtained, and new kind of ceramics have been reported.^[22]

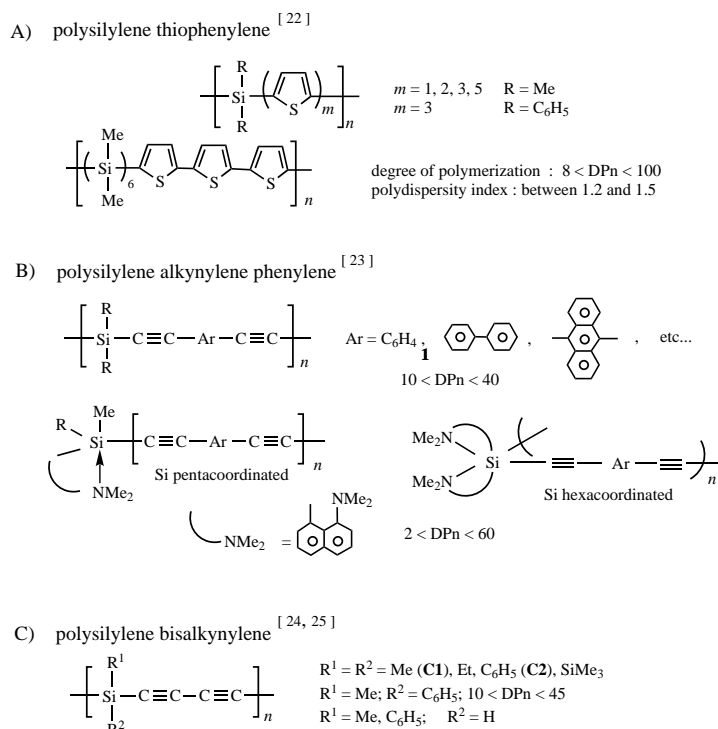


Scheme 4. The one-pot, rheologically controlled pathway to SiC, shown with the example of 1,4-disilapentane (**II**).

3. Elaboration of Ceramics in a Carbon Matrix: Access to Nano-Composite Mixed Ceramics

3.1. Silicon-Containing Polymers: Synthesis and Conductivity

In the course of our work concerning the synthesis of silicon-containing polymers, we have prepared three sets of polymers in which -(SiR₂)- units bridge unsaturated organic units (Scheme 5). After doping, all these polymers exhibit conductivity in the range of 10⁻³ to 10⁻⁶ S cm⁻¹.^[23-28] The materials in Scheme 5B offer second (χ₂)^[24c] and third harmonic (χ₃) nonlinear optic properties.^[24c,d]



Scheme 5. Silicon-containing polymers obtained in the author's laboratory.

The case of polysilylene bisalkylene (Scheme 5C) is interesting since, although the acetylenic units are not favorable to conduction,^[25] these polymers exhibit conductivities between 10⁻⁵ and 10⁻³ S cm⁻¹. Furthermore, the values are dependent on the groups attached to silicon. The highest values (3 × 10⁻³ S cm⁻¹) are obtained with Ph₂Si, the lowest with Me₂Si (8 × 10⁻⁵ S cm⁻¹). This observation is in agreement with an electronic interaction induced by silicon atoms which favors charge delocalization. A possible explanation corresponding to a chain-to-chain conduction mechanism can be eliminated since, in this hypothesis, the highest values should be obtained with the dimethyl polymer **C1**, which exhibits the best crystallinity^[29] and the shortest distance between the acetylenic chains (4.6 Å). In contrast, the phenylated polymer **C2** should

exhibit a lower conductivity since the steric hindrance, which increases the repulsion between the polymeric chains, should prevent the chain-to-chain conduction mechanism. The experimental results clearly show that aromatic substituents at silicon are the best for increasing the conductivity.

3.2. Ceramization of Polydimethylsilylene Bisalkylene

The dimethylated polymer **C1** (see Scheme 5) was pyrolyzed under argon.^[30] Surprisingly, a residue was obtained that was analyzed as having a composition ratio of Si/5C. On heating to 1400 °C, β -SiC crystallizes, and the analysis corresponds to SiC/4C. During pyrolysis no gaseous products containing silicon were eliminated: Only CH₄ and H₂ were formed (Figure 1).

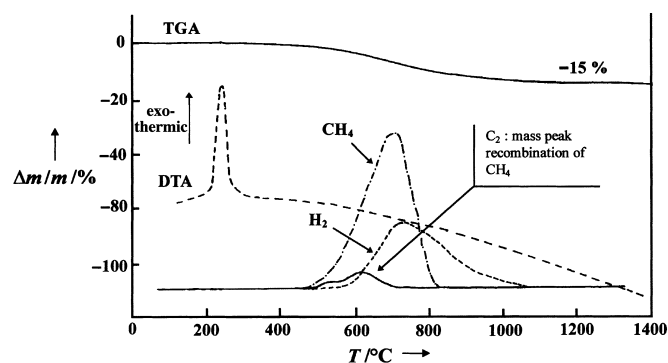
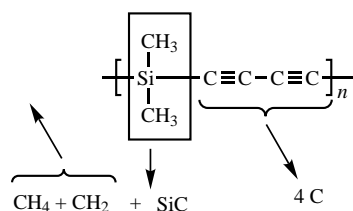


Figure 1. Thermal and gas analyses in the pyrolysis of polymer **C1**. m = mass, DTA = differential thermal analysis, TGA = thermogravimetric analysis.

Differential thermal analysis (DTA) exhibits a sharp exotherm at 200 °C (Figure 1). This exotherm takes place before the evolution of CH₄ (450 °C) and H₂ (550–600 °C). Given that linear precursor polymers depolymerize into short volatile units during pyrolysis, a cross-linking process is always necessary to obtain ceramics in good yields.^[14, 31, 36] Taking this fact into account and considering the results obtained by elemental analysis, thermogravimetric analysis (TGA), and DTA, the best working hypothesis is that presented in Scheme 6: The 4C residue should originate from the bisacetylenic units, and the SiC should form from SiMe₂ groups with concomitant elimination of CH₄ and H₂. In other words the exothermic transformation observed at 200 °C should correspond to the formation of a carbon matrix by 1,4-addition of bisacetylenic units, as already observed in related systems.^[32] This transformation is likely the key step leading to a cross-linked material which aids the formation of SiC.



Scheme 6. Mechanistic hypothesis for formation of SiC from **C1**.

As a chemical proof, we checked that the formation of SiC correlates with the presence of bisacetylenic units in the molecule: The saturated polymer [Me₂Si(CH₂)₄]_n does not form SiC, and the semisaturated polymer [Me₂Si(CH₂)₄SiMe₂C≡C-C≡C]_n provides less than 40% of the theoretical amount of SiC.^[29] In the case of polymer **C1**, the formation of the carbon matrix was detected by both IR and ¹³C CP-MAS NMR spectroscopy (CP-MAS = Cross-polarization magic angle spinning), which shows the transformation of sp into sp² carbon atoms, corresponding to the transformation of C≡C-C≡C units into enynes and butatrienes at 200 °C and then final formation of the sp²-carbon matrix above 400 °C.^[30]

In agreement with this explanation, we observed that the exothermic transformation is highly dependent on the steric hindrance of the groups attached to silicon. In the case of **C1**, the X-ray diffraction (XRD) pattern reveals the presence of a lattice in which the repeat distance of the diacetylene backbone is 4.6 Å.^[29, 30] The crystallinity decreases in the order Me > Ph > SiMe₃, as observed by XRD, and the temperature of cross-linking follows the same order (Me: 200 °C, Ph: 225–315 °C, SiMe₃: 350 °C; Figure 2).

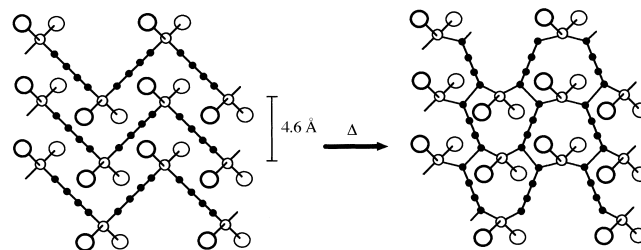


Figure 2. Representation of the cross-linking process.

This cross-linking reaction between the C≡C-C≡C chains explains why the isolated dimethylsilyl units react with each other to form a SiC network. Although the SiMe₂ groups are chemically isolated, they are in a fixed geometric position inside of the carbon matrix—this permits their reaction with elimination of H₂ and CH₄. In this case, the cross-linking reaction does not occur between functionalities at SiC. A mechanism that can be proposed for the ceramization is presented in Scheme 7.^[30]

The initiation step is the formation of a CH₃· radical by cleavage of a Si-CH₃ bond. The abstraction of H· leads to evolution of CH₄ and formation of a SiCH₂· radical, which permits the formation of SiCH₂Si units and regeneration of CH₃· (propagation step).

The evolution of H₂ takes place at higher temperature (>500 °C). It can be explained by cleavage of C-H bonds followed by reaction of the Si·CHSi radical on a Si atom located in the vicinity. This reaction occurs with cleavage of the bond linking this Si atom to the unsaturated cross-linked carbon matrix. In this way, the SiC network is formed from the (SiCH₂Si) units.

Whatever the substituents are at silicon (SiMe₂, SiEt₂, Si(C₆H₅)Me, Si(C₆H₅)₂), the conservation of Si and its transformation into SiC is high (95–99%). Furthermore, when the

3.4. Mechanism of Formation of Mixed Carbides

The effect due to the carbon matrix and its formation around the oxide particles is the driving force of these processes. A chemical proof can be afforded by comparing the results of ceramization by mixing the oxide before or after formation of the carbon matrix. In the case of TiO_2 and ZrO_2 complete carbothermal reduction is observed when the carbon matrix is formed in the presence of the oxide particles. However, in the second procedure (mixing the oxide with the cross-linked polymer) 30% of TiO_2 and 70% of ZrO_2 are not transformed into TiC or ZrC .

Transmission electron microscopy performed after the cross-linking step shows the TiO_2 grains embedded inside the carbon matrix (Figure 4). Moreover, after treatment at 800°C the TiO_2 is not modified and nanoparticles corresponding to SiC are visible. The fact that the oxide particles are closely embedded by the carbon matrix explains the lower temperature observed for the carboreduction with respect to the values reported in the literature.

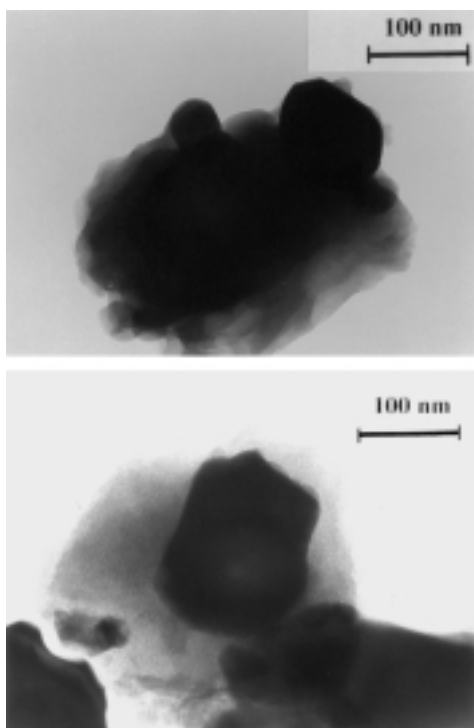
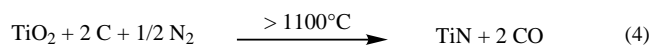


Figure 4. Transmission microscopy for a) $\text{TiO}_2/\text{C1}$ at 300°C and b) $\text{TiO}_2/\text{SiC}/4\text{C}$ at 800°C .

3.5. Preparation of Mixed SiC–Metal Nitrides

It is well known that the carbothermal reduction of some metal oxides under N_2 gives nitrides.^[36] This reaction occurs at temperatures above 1100°C , as illustrated for TiO_2 [Eq. (4)].^[38]



We performed the ceramization under a flow of nitrogen and observed the formation of residues corresponding to mixed ceramics of SiC and metal nitrides^[34–39] (Table 2). Interestingly, materials are obtained with ceramic yields quite close to the expected values. In every case, reactions occur at lower temperatures and with a higher rate than reported in the literature.^[36]

Table 2. Synthesis of SiC –metal nitride ceramics by pyrolysis of **C1** and metal oxide dispersions under a nitrogen flow.

Equiv of polymer	Metal oxide (equiv.)	Ceramic yield [%] ^[a]	Stoichiometry of the ceramic ^[b] (MN [%])
1	TiO_2 (2)	64 (62)	$\text{SiC}/2\text{TiN}$ (75.6)
1	ZrO_2 (2)	66 (71)	$\text{SiC}/2\text{ZrN}$ (84.0)
1	HfO_2 (2)	84 (81)	$\text{SiC}/2\text{HfN}$ (90.6)
5	V_2O_5 (4)	58 (57)	5 $\text{SiC}/8\text{VN}$ (72.2)
5	Nb_2O_5 (4)	71 (66)	5 $\text{SiC}/2\text{Nb}_4\text{N}_{3.92}$ (81.0)
3	B_2O_3 (4)	49 (53)	3 $\text{SiC}/8\text{BN}$ (62.3)
3	Al_2O_3 (4)	62 (62)	3 $\text{SiC}/8\text{AlN}$ (73.2)
1	SiO_2 (2)	62 (59)	$\text{SiC}/\frac{2}{3}\text{Si}_3\text{N}_4$ (70.0)

[a] Theoretical values are given in parentheses. [b] Determined by IR spectroscopy and XRD. MN = analytical results of the metal nitride.

The mixture of a carbide and a nitride is also possible since these two kinds of ceramics can be obtained by different chemical routes. Degradation under nitrogen of the polymer **C1** leads only to SiC , and the formation of metal nitrides takes place at a higher temperature. In the case of metals like Ti and Zr , the most reasonable explanation is the direct reaction of nitrogen with the metal.^[34b), 36, 38, 39] However, in the case of silicon, Si_3N_4 formation can result from the reaction of N_2 with low oxides (compounds with low oxide content) formed as intermediates during the carbothermal reduction, since it is well established that Si_3N_4 cannot be obtained by reaction of nitrogen with the polymer or with SiC in this temperature domain. The identification was carried out by XRD; Figure 5 shows an example for the β - SiC and hexagonal HfN ceramic.

Thus, as shown in Scheme 8, the mechanism of carbothermal reduction takes place with initial formation of metal oxides and/or low oxides as intermediates.^[36, 38] When the transformation is performed under argon, the excess of carbon reacts with these intermediates, leading to metal

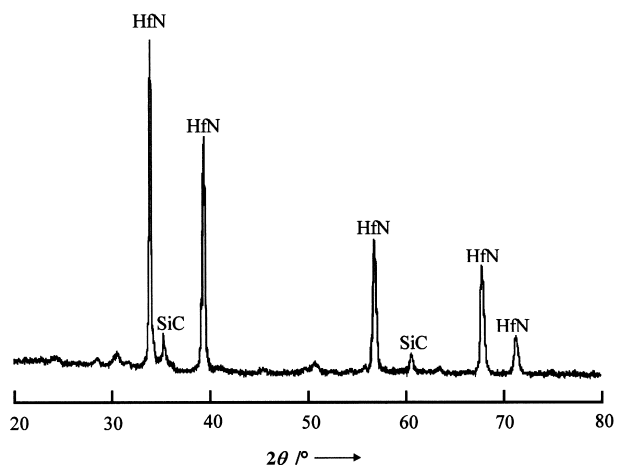
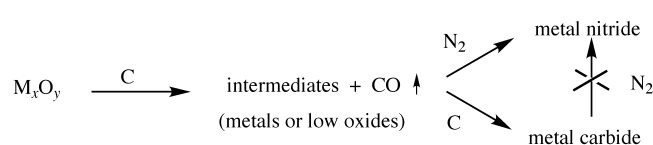


Figure 5. X-ray diffraction pattern of a SiC – HfN ceramic.



Scheme 8. Proposed mechanism for metal nitridation.

carbide. In contrast, under a nitrogen atmosphere the reaction with the metal (or in some cases with low oxides) is faster since 1) the gas/solid contact is more efficient than the solid/solid contact and 2) the products are thermodynamically more stable.^[36] Only metal nitrides are obtained under these conditions; no nitrides are assumed to be formed by the reaction of nitrogen with carbides.

3.6. The Nature of the Mixed Ceramics Obtained

The oxide powders used for the ceramization studies were submicron powders. The analyses show that the distribution of particle sizes is wider in the final material than in the starting material. The IR spectra demonstrate clearly that the silicon is present only as SiC (830 cm^{-1})—neither SiO_2 ($1000\text{--}1200\text{ cm}^{-1}$)^[40] nor any other oxide (TiO_2 , ZrO_2 , etc...) is observed.

As an example, the XRD pattern of the ceramic resulting from pyrolysis of polymer C1 and Nb_2O_5 under argon shows only carbides ($\beta\text{-SiC}$ and NbC), corresponding to complete carbothermal reduction of the oxides (no oxide is detected by FT-IR spectroscopy and XRD at the end of the process; Figure 6). The XRD pattern shows that SiC is formed in

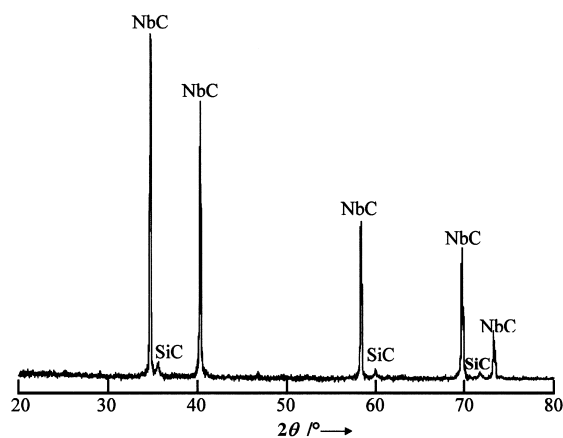


Figure 6. X-ray diffraction pattern of a SiC-NbC ceramic.

addition to the carbides (or the nitrides). However, its signals are broader and weaker than those of the carbides (or the nitrides) resulting from the carbothermal reduction. We can conclude that both ceramics are present as separated phases. However, the crystalline domains resulting from carbothermal reduction are larger than the $\beta\text{-SiC}$ crystals, as easily observed in transmission electron microscopy.

A solid solution or an alloy can be excluded as a possible structure since the XRD diagrams of both the components are observed. The two possibilities are now either a mixture

consisting of particles of SiC beside particles of other carbides (or nitrides), or particles containing the two kinds of ceramics. In order to discriminate between the two, we considered the EDAX diagram of the particles (Figure 7). This diagram shows that the ratio of Si to metal is identical to the ratio introduced in the starting material. Furthermore, this ratio is quite constant at each point of one particle and for all the particles considered.

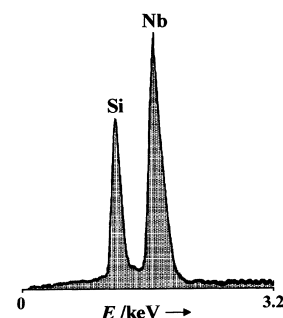


Figure 7. EDAX spectrum of a SiC-NbC ceramic showing retention of the initial Si:Nb ratio (7:8) in the final material.

All these results show that we are faced with a ceramic structure which cannot be described as an alloy since we could not observe the XRD patterns for both components. However, the ceramics obtained are not a mixture of particles of $\beta\text{-SiC}$ and particles of the other metal carbide (or nitride). We observe an intermediate situation in which the powder is chemically homogeneous, all particles exhibiting the same chemical composition. However, it is possible to detect crystalline components, showing that each particle is an agglomerate of crystals of both $\beta\text{-SiC}$ and the carbide (or nitride) resulting from carbothermal reduction. The alloy is not formed since the crystals do not have the same crystalline variety and since the rather low temperature does not permit alloy formation or phase separation.

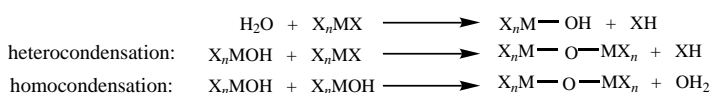
By comparison with the case of mixing polymers,^[41] the ceramic obtained could be described as a mixed ceramic with interpenetrating networks. However, following the terminology proposed in ceramic science, the term nanocomposite ceramic^[42] seems more appropriate.

In conclusion, the results described in Section 3 show that the molecular approach to materials permits one to obtain solid materials that have not been reported previously. These nanocomposite ceramics or interpenetrating networks^[42] are accessible only by a step-by-step kinetic preparation and by controlling the chemistry throughout the process. Thus $\beta\text{-SiC}$ (cubic diamond) is formed at a rather low temperature (below 800°C). The carbothermal reduction gives the second ceramic at a temperature which does not permit the transformation of $\beta\text{-SiC}$ into $\alpha\text{-SiC}$ (hexagonal). Moreover, since these transformations are performed in the carbon matrix obtained by the cross-linking of C_4 units, the two ceramics are maintained in the same particle without any thermodynamic transformation. This situation was never described before and it can be obtained only by a kinetic route.

4. Sol–Gel Chemistry

The “chimie douce”^[11, 12] methods include the sol–gel processes,^[13] which correspond to hydrolytic polycondensations in which the leaving groups at the metal are substituted by nucleophilic attack of H_2O , followed by elimination of the leaving group and formation of a metal hydroxyde. This in

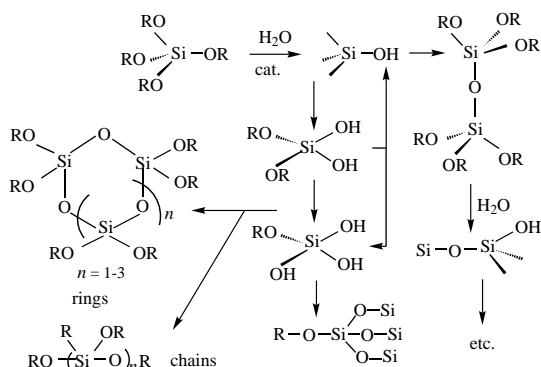
turn leads to metal oxide bonds either by homo- or heterocondensation^[43] (Scheme 9).



Scheme 9. Hydrolytic condensation of metal alkoxides.

Hydrolytic polymerization is a general process that occurs at many metal centers and makes use of many different leaving groups: X can be, among others, halide, sulfide, alkoxide, or nitride. However, the most widely used are the alkoxides and the most intensively studied element is silicon, which leads to silica.^[44, 45]

It is important to point out that polycondensation is always a very complex mechanism, even for SiO₂ formation, which is considered the most simple process.^[46] Scheme 10 illustrates this complexity, at least in the first steps. When polycondensation goes further, the situation becomes even more complex since many reactions occur in competition: redistribution, ring closure, and ring opening. Finally, colloids form, leading to sol production. The coalescence of these colloids at the gel time leads to formation of xerogels.



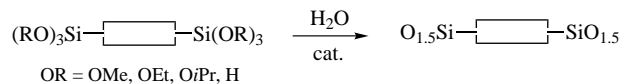
Scheme 10. Illustration of the chemical complexity of sol-gel hydrolytic polycondensations.

Importantly, the details of the polymerization mechanism are not well known, and only few reliable kinetic data have been reported concerning the first steps.^[47] Moreover, it is difficult to compare the sets of experiments reported in the literature since most authors use pH as a measure of medium acidity or basicity although it is well known since the work of Hammet and Deryup that only the H_0 functions are valid when the experiments are carried out in aqueous-organic media.^[48] Moreover it was established that the solid is formed after a set of very complexed steps:^[13b] precursor \rightarrow oligomers \rightarrow polymers \rightarrow colloids \rightarrow sol \rightarrow gel. Thus it is impossible to predict the properties of the final solid, since the nature and the degree of influence of the parameters controlling each step are not known.

However, despite the lack of precise knowledge concerning the details of the mechanisms of gel formation, this field of research is very attractive because it opens wide possibilities for the preparation of materials. Scheme 11 illustrates the

high efficiency of sol-gel processes for the elaboration of solids. This method is particularly attractive for molecular chemists since elaboration can be performed at room temperature under the same experimental conditions used in organic or inorganic chemistry. There is why these processes have been named “chimie douce”.^[11, 12]

In previous reviews, we have described the sol-gel chemistry of new kinds of precursors and nonhydrolytic gelation methods.^[13g, 49] The present article focuses on organic-inorganic hybrid materials.^[49-55] The number of investigations performed on this topic is growing very quickly and the possibilities are wide open. More precisely, Section 5 will be devoted to the elaboration of nanostructural materials (nanostructures) by building up an inorganic matrix around an organic unit starting from a molecular precursor used as a building block (Scheme 12).

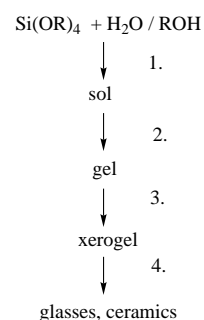


Scheme 12. A method for elaboration of nanostructural materials from molecular precursors.

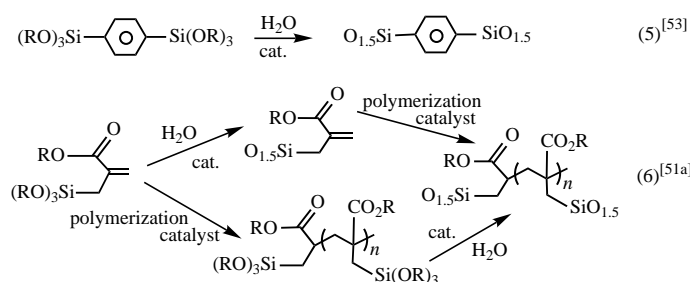
5. Organic-Inorganic Hybrid Materials: Scope and Limitations

5.1. Nanostructural (Monocomponent) and Nanocomposite (Polycomponent) Hybrid Materials

The phrase “organic-inorganic material” is used widely and covers many kinds of solids. The greatest possibilities are available to polycomponent materials that are generally obtained by mixing organic molecules or polymers with metal alkoxides. The materials are obtained by polycondensation of the alkoxides into oxides using sol-gel methods. Although most of these systems appear homogeneous (single phase), they correspond to a polycomponent system since they can be separated into two phases by classical separation techniques (washing with an organic solvent, for instance). In contrast, all systems in which the components are bound by covalent bonds exhibit different behavior. Whatever separation methods are used, they always appear as a homogeneous single phase: They cannot be separated by analytical techniques since all atoms are covalently bound. For instance, one hybrid prepared by polycondensation with a molecular precursor as a building block^[53] (Scheme 13, reaction (5)) and another obtained by polymerization of organic units inside an oxide matrix^[51a] (reaction (6)) are both monocomponent systems, and can be considered as nanostructured materials. However, it is obvious that the two materials are very different with respect to homogeneity and short- to medium-range organ-



Scheme 11. General scheme of the sol-gel process: 1. hydrolysis/condensation; 2. sol-gel transition; 3. drying; 4. densification.



Scheme 13. Two possible pathways to monocomponent solids. cat. = H⁺, OH⁻, F⁻.

ization in the solid. Furthermore, in the case of reaction (6), the two possible routes provide very different solids. When the polymerization is the first step, the material contains polymeric chains cross-linked by hydrolytic polycondensation of Si(OR)₃ groups. When polycondensation is the first step, polymerization leads to the linkage of R–SiO_{1.5} clusters.

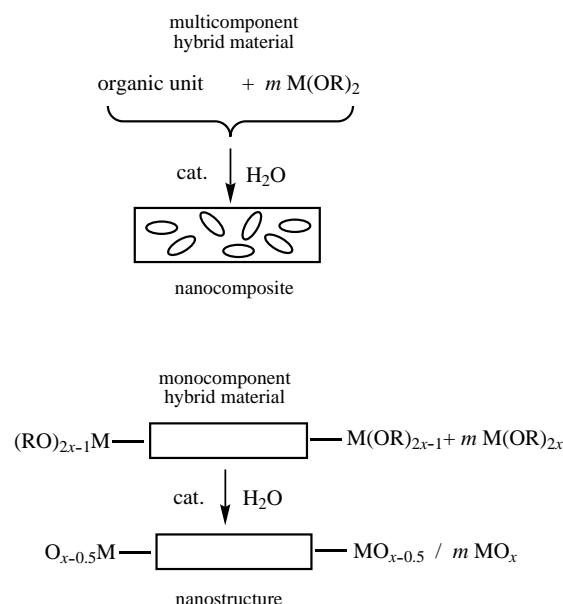
In contrast, hybrid materials obtained by mixing organic moieties with one (or more) alkoxide precursors correspond to nanocomposites after formation of oxides by precursor polycondensation.^[50, 51] These solids can be separated into different components by classical separation techniques, for instance, washing of the solid. The term nanocomposite seems the most appropriate for them.

It is important to point out that Gibb's rule is difficult to apply here since all these solids form under kinetically controlled conditions (see Section 6). They are far away from equilibrium and cannot be described as stable phases. Most of these solids are not crystalline and behave as amorphous materials with a morphology whose evolution depends on the experimental conditions.

This review is devoted to those nanostructural materials (or nanostructures) that correspond to monocomponent hybrid organic–inorganic solids elaborated from a molecular precursor used as a building block, and are designed to permit hydrolytic polycondensation around the organic unit (Scheme 14). More precisely, the preparation of monocomponent hybrid materials following Scheme 14 is determined by the chemistry of the building block. The first condition is the existence of nonhydrolyzable and nonoxidizable covalent bonds between the organic unit and the oxide matrix. The second condition is the presence in the building block of M(OR)_{2x-1} groups that allow formation of the oxide matrix by hydrolytic polycondensation.

Silicon chemistry provides one of the best solutions to this problem. The use of a Si–C bond brings a stable link between the organic unit and the oxide matrix. The presence of a trifunctional silicon atom (SiX₃) provides access to the SiO₂ matrix by hydrolytic polycondensation. Trialkoxysilyl groups Si(OR)₃ (R = Et, Me, *i*Pr) are used most commonly.^[53–55] However, SiCl₃^[56] and SiH₃ groups^[57] can also lead to silica matrices.

Interest in silicon is also based on the very facile formation of silicates and polysiloxanes by hydrolysis of functional groups at silicon. Moreover the Si–C bond is highly resistant to hydrolysis and oxidation. Finally, the organic chemistry of silicon has been widely developed, and provides many chemical ways to introduce silicon-containing groups in an



Scheme 14. Schematic illustration of the difference between nanostructures and nanocomposites. In the case of nanocomposites (top) the organic units are embedded in the oxide matrix and can be separated from the matrix. For nanostructures (bottom; the rectangle represents a building block) a homogeneous system is formed in which the organic units are bound to the matrix and therefore nonseparable.

organic molecule^[58] for the synthesis of molecular building blocks.

This section focused on nanostructural materials obtained from precursors containing at least two Si–C bonds. The case of monocomponent hybrids with only one Si–C bond will be discussed separately (Section 5.2).

5.2. Monocomponent Hybrids with Only One Si–C Bond

This case is the most commonly studied since monocomponent systems provide functionalized surfaces that are very useful for catalysis or separation technologies.^[59] This field was reviewed recently.^[52]

It is interesting that here the organic part of the precursor is located mainly at the surface after the solid forms. This fact can be demonstrated by time-of-flight secondary ion mass spectroscopy (TOF-SIMS). In all cases studied, TOF-SIMS permits detection of specific organic fragments.^[60] Some examples are given in Table 3.

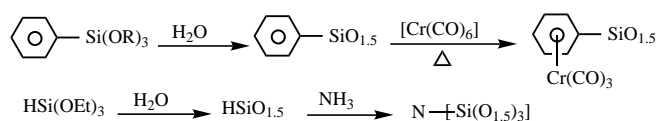
The TOF-SIMS data can be corroborated by other experimental data, such as the hydrophilicity and/or chemical reactivity. The fact that the hydrophilicity of silsesquioxanes (R–SiO_{1.5}) is poor is easily explained by the presence of hydrophobic organic groups at the surface of the solid, instead of hydrophilic OH groups expected for SiO₂.^[60, 61, 63]

The chemical reactivity corroborates these facts: R groups located at the surface are chemically accessible and highly reactive. Two examples are the facile complexation of phenyl groups by Cr(CO)₃ in phenyl silsesquioxanes,^[62] and the transformation of HSiO_{1.5} into oxynitride by reaction in a simple flow of NH₃^[63] (Scheme 15).

Table 3. Main ions observed in the time-of-flight secondary ion mass spectra (TOF-SIMS) of various gels.^[a]

Hybrid gel	Ions
CH ₃ SiO _{1.5}	15 (CH ₃) ⁺ , 43 (SiCH ₃) ⁺
ICH ₂ CH ₂ CH ₂ SiO _{1.5}	127 I ⁺ , 141 (ICH ₂) ⁺ , 155 (ICH ₂ CH ₂) ⁺ (negative ions: 127 I ⁻ , 254 I ²⁻)
H ₂ NCH ₂ CH ₂ CH ₂ SiO _{1.5}	30 (CH ₂ =NH ₂) ⁺ , 44 (H ₂ NCH ₂ CH ₂) ⁺
[1-(NMe ₂ CH ₂)-2-(SiO _{1.5})]C ₆ H ₄	58 (CH ₂ =NMe ₂) ⁺ , 134 (C ₆ H ₅ CH ₂ NMe ₂) ⁺
C ₆ H ₅ NHCH ₂ CH ₂ CH ₂ SiO _{1.5}	106 (CH ₂ =NHC ₆ H ₅) ⁺
(C ₆ H ₅) ₂ PCH ₂ CH ₂ SiO _{1.5}	109 (C ₆ H ₅ PH) ⁺ , 123 (C ₆ H ₅ PCH ₂) ⁺
Fe[(η ⁵ -(C ₅ H ₄)(SiO _{1.5}))][η ⁵ -C ₅ H ₅]	183 (C ₁₂ H ₈ P) ⁺ , 185 [(C ₆ H ₅) ₂ P] ⁺
Fe[(η ⁵ -(C ₅ H ₃)(SiO _{1.5})(CH ₂ NMe ₂))][η ⁵ -C ₅ H ₅]	56 Fe ⁺ , 121 (C ₅ H ₅ Fe) ⁺ (negative ions: 65 (C ₅ H ₅) ⁻)
Fe[(η ⁵ -(C ₅ H ₃)(SiO _{1.5})(CH ₂ NMe ₂))][η ⁵ -C ₅ H ₅]	56 Fe ⁺ ; 58 (CH ₂ =NMe ₂) ⁺ ; 121 (C ₅ H ₅ Fe) ⁺

[a] The major fragments are shown in bold characters.



Scheme 15. Chemical evidence for the surface location of organic groups.

5.3. Identification of Nanostructural Materials

The identification of the hybrid materials must be considered at three levels: The first level is the classical identification of the solid in terms of macroscopic data (granulometry, specific surface area, porosity, density, hydrophilicity, etc.). This set of experimental data permits one to characterize the *texture* of the material, which corresponds to a macroscopic description of the amorphous solid.

However, in the case of nanostructured hybrid materials, a microscopic aspect of characterization must be taken into account. There is the *molecular* level, which corresponds to the presence of the organic part in the solid and to the degree of polycondensation around the silicon atom. Moreover, organic moieties can exhibit a short- to medium-range order in the solid. There is the *structural* level, reflecting the possible relative arrangement of the organic units within the solid.

These three levels will be discussed successively. Sections 6 and 7 will deal with the identification of the texture of the material as well as the

evidence connected to possible structural organization within the solid.

Let us consider identification at the molecular level: Solid-state ¹³C NMR spectroscopy is a means of identifying the molecular units present in the solid, while ²⁹Si NMR spectroscopy provides information about the degree of polycondensation of the silica network. For example, two different precursors **D** and **E** can be used for the elaboration of two nanostructural materials; **E** is obtained by treatment of **D** with [Cr(CO)₆] (Scheme 16). After polycondensation the nanostructures **D'** and **E'** are formed from **D** and **E**.^[57b, 64] ²⁹Si CP-MAS NMR spectroscopy permits one to determine the degree of polycondensation (T^y) at silicon (Figure 8) and to show that this degree is highly dependent on experimental conditions (see Section 6). It is interesting that this method may allow quantitative evaluation when cross-polarization is not used.^[65] ¹³C CP-MAS NMR spectroscopy permits assignment of all the carbon atoms of the organic moiety.

A second example for the use of solid-state ¹³C and ²⁹Si NMR spectroscopy is as follows: In the course of our studies concerning the controlled elimination of organic units from

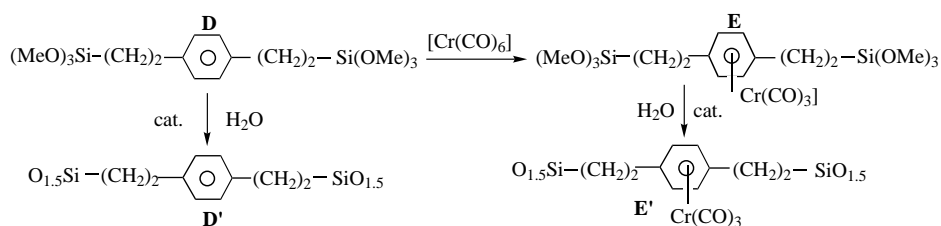
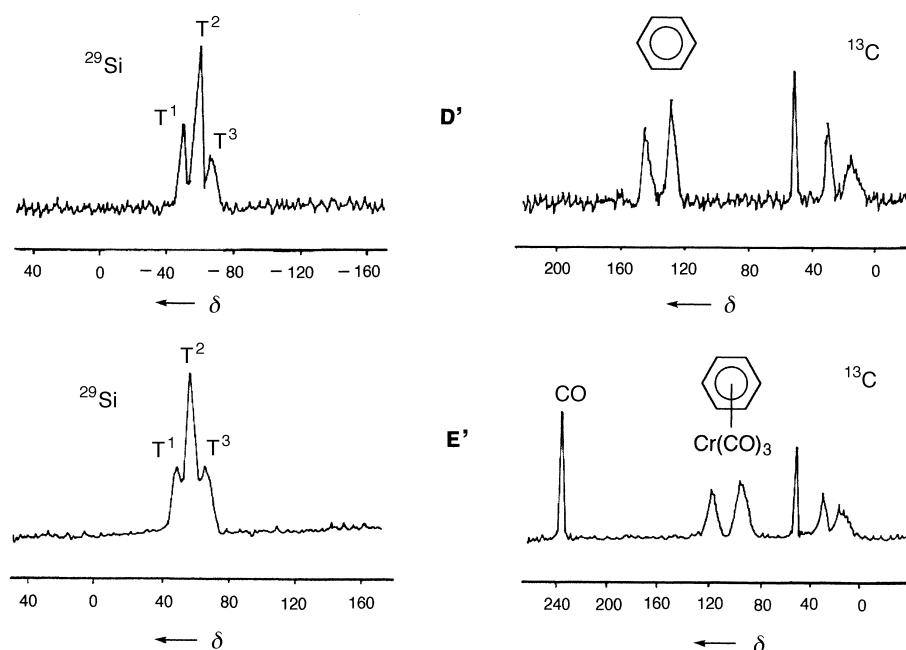
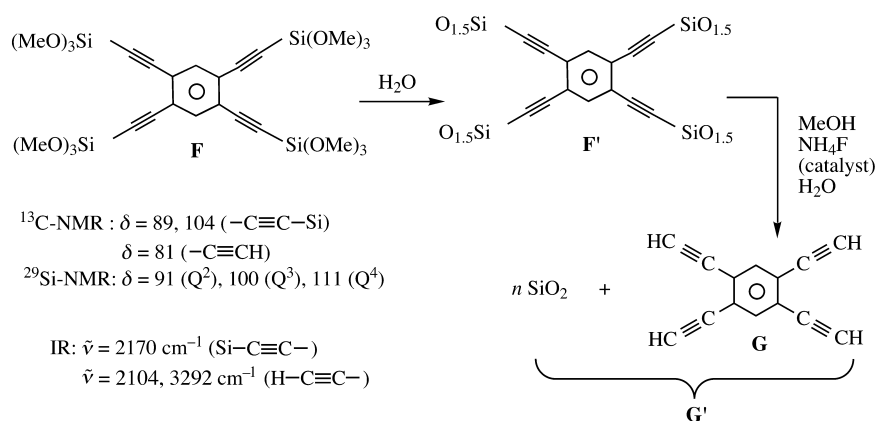
Scheme 16. Preparation of the nanostructured materials **D'** and **E'**.

Figure 8. The ²⁹Si and ¹³C CP-MAS NMR spectra of **D'** and **E'**. The T^y value (degree of polycondensation) of a carbon-bound Si center describes the number of tetrahedra: C-Si(OSi)_y(OR)_{3-y} with SiOSi bonds.

Scheme 17. Identification of molecule **G** encapsulated in silica.

hybrid materials, we used polyethynylated aromatic systems, which permit chemically induced selective elimination of the organic unit when NH_4F is used as catalyst^[57] (see Section 8). Scheme 17 shows the case of a tetraethynylbenzene. From precursor **F** the nanostructural material **F'** is obtained by hydrolytic polycondensation. After treatment with NH_4F as catalyst (2%) in the presence of MeOH and H_2O , the molecule **G** is formed.^[66]

Surprisingly, **G** could not be separated from SiO_2 regardless of the separation technique used. However, the IR and NMR features of solid **F'** and solid **G'** (silica-containing **G**) permit unambiguous identification of cleavage of the $\text{Si}-\text{CC}$ bond and the presence of **G** inside the silica matrix. The complete transformation of T units into Q units is particularly illustrative and obvious in the ^{29}Si NMR spectrum.^[65] (The Q^x value of a Si center describes the number of directly bound SiO_4 tetrahedra: $\text{Si}(\text{OSi})_x(\text{OR})_{4-x}$, $x=0-4$; the T^y value is analogous for carbon-bound Si centers: $\text{C}-\text{Si}(\text{OSi})_y(\text{OR})_{3-y}$, $y=0-3$.) The disappearance of signals for $\text{SiC}\equiv\text{C}$ and the presence of $\text{HC}\equiv\text{C}$ characteristics are also evidenced by IR and ^{13}C NMR spectroscopy (Scheme 17).

In conclusion, in all cases studied until now, the organic unit is always attached to the silica network without any transformation.^[53-55] The $\text{Si}-\text{C}$ bond is stable enough to provide a homogeneous nanostructural material in which the organic moieties bound to two $\text{SiO}_{1.5}$ units are distributed as elementary building blocks. Solid-state NMR spectroscopy permits one to verify that the building blocks are not chemically modified during elaboration of the solid.

The only case where $\text{Si}-\text{C}$ bond cleavage is observed is when $\text{Si}-\text{C}\equiv\text{C}$ single bonds are cleaved by nucleophilic attack of H_2O promoted by nucleophilic activation by F^- .^[57] This will be discussed in Section 8.

^{29}Si NMR spectroscopy, which reflects the degree of polycondensation, exhibits very great differences between the solids, depend-

ing to a large part on the nature of the organic unit. This point will be discussed in more detail in Section 6.

Most of the nanostructural materials that have been obtained and identified to date are presented in Scheme 18. The bisacetylenic structures will be described in Section 8.

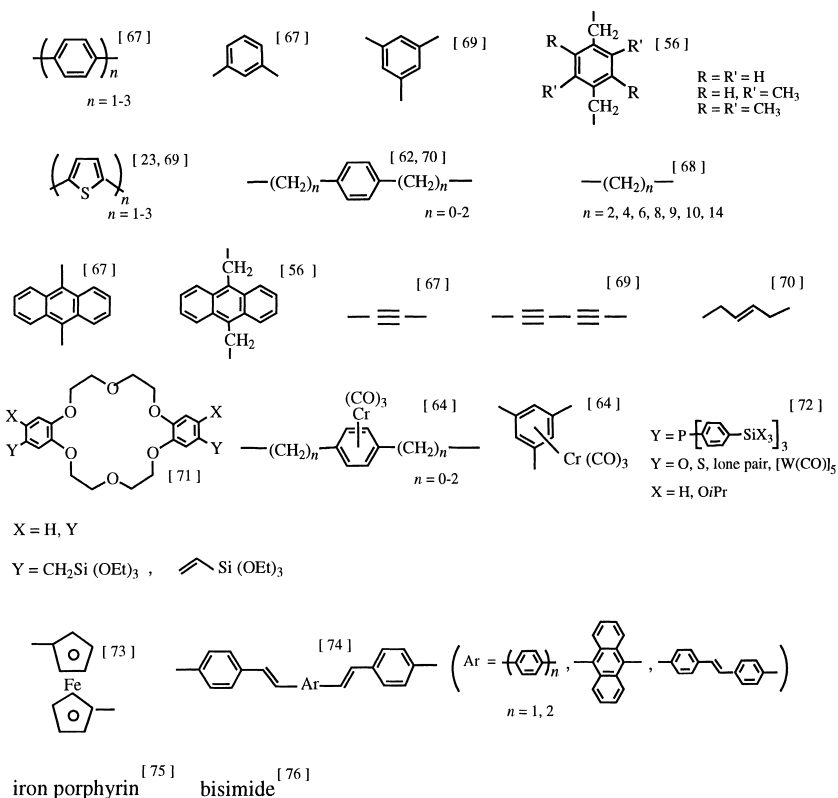
5.4. Identification of the Solid

The identification of solids is divided into two parts: The first corresponds to the macroscopic data that permit a description of the texture of the solid, for example specific surface area, granulometry, porosity, density, and hydrophilicity. This aspect will be discussed in Section 6 with regard to kinetic control of the solids. The structural description of the solid corresponding to the interactions between the organic units and the possible organization in the solid will be discussed in more detail in Section 7.

6. Nanostructural Materials: Kinetic Control of the Formation of the Solid

6.1. Control of the Texture by Kinetics

It is well known that the texture of oxide materials obtained by sol-gel methods is highly dependent on the experimental



Scheme 18. Examples of organic units included in nanostructured materials.

conditions.^[43–47] Among others, the gelation time, specific surface area, porosity, and granulometry change with all the parameters used for hydrolytic polymerization (e.g. concentration of reagents and catalyst, solvent). The solids obtained are described as thermodynamically unstable materials.^[43]

In the case of nanostructures obtained from building blocks, the effect is more drastic since the nature of the organic moiety plays an important role in the polycondensation reaction and since polymerization occurs on six SiX groups in the case of bisilylated precursors (or more when tri- or polysilylated precursors are used). The texture of the solid is controlled by all the parameters able to modify the kinetics of polycondensation. This is illustrated by several examples in Table 4, in which the texture is shown to be a function of catalyst,^[77a,b] concentration of the reagents,^[77a,b] leaving groups,^[56, 57] organic spacer,^[77a,b] solvent,^[77a,b] and temperature.^[77a]

These results illustrate very well the very narrow connection between the macroscopic data that describe the texture of the solid and the microscopic parameters controlling the kinetics of all the chemical reactions involved in the elaboration of the solid: hydrolytic polycondensation leading to the colloids (sol formation) and cross-linking reactions transforming the sol into a gel.^[77]

Kinetic control is also illustrated by the effect of catalyst type on the degree of polycondensation, as measured by ²⁹Si

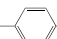
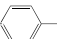
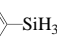
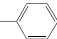
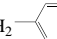
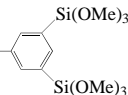
NMR spectroscopy. Figure 9 shows, for instance, the great difference in the solid obtained simply by changing the counterion used in nucleophilic catalysis; all other parameters were identical.^[64, 77]

All these experiments are reproducible. However, the reproducibility in texture and polycondensation is obtained only when the experimental conditions (including the purity of chemicals) are carefully controlled.

6.2. Effect of Weak Interactions on the Organization of the Solid

Another interesting example of the close relationship between the texture of the material and the kinetic parameters is the effect due to weak interactions. In the case of SiO₂, the effect of weak interactions is best illustrated by the preparation of silicas with a controlled pore size and shape through the use of surfactants and micellar media. In the case of hybrid systems, this effect can be best understood by studying solid formation using charge transfer complexes. It is known that terthiophene and 7,7,8,8-tetracyano-*p*-quinodimethane (TCNQ) form such complexes.^[78] As illustrated in Scheme 19, bis(trimethoxysilyl)terthiophene (**H**) gives charge complex (**I**) upon reaction with TCNQ.^[23c] By cohydrolysis with Si(OMe)₄, a solid (**J**) is obtained, which exhibits a poor

Table 4. Relationship between kinetic parameters and the texture of the hybrid materials.

Precursor	<i>c</i> [mol L ⁻¹]	Solvent	Catalyst ^[a]	<i>t</i> ^[b] [min]	<i>S</i> ^[c] [m ² g ⁻¹]
(MeO) ₃ Si—  —Si(OMe) ₃	0.5	MeOH	NH ₄ F (10 ⁻²)	60	558
	1	MeOH	Bu ₄ NF (10 ⁻²)	4	1050
	0.5	MeOH	Bu ₄ NF (10 ⁻²)	160	550
	1	THF	Bu ₄ NF (10 ⁻²)	4	1240
	0.5	THF	Bu ₄ NF (10 ⁻²)	135	370
	0.5	THF	NH ₄ F (10 ⁻²)	10	388
(MeO) ₃ Si(CH ₂) ₂ —  —(CH ₂) ₂ Si(OMe) ₃	0.5	MeOH	Bu ₄ NF (10 ⁻²)	720 ^[d]	< 10
	0.5	MeOH	Bu ₄ NF (10 ⁻²)	45	< 10
	1	MeOH	Bu ₄ NF (10 ⁻²)	10 ^[d]	< 10
	0.5	THF	Bu ₄ NF (10 ⁻²)	< 5	565
	1	THF	Bu ₄ NF (10 ⁻²)	2	531
	0.5	THF	NH ₄ F (10 ⁻²)	3900	< 10
H ₃ Si—  —SiH ₃	0.5	THF	Bu ₄ NF (10 ⁻³)	300	931
	1	THF	Bu ₄ NF (10 ⁻³)	0.2 ^[e]	1200
	0.5	THF	[(Ph ₃ P) ₃ RhCl] (10 ⁻³)	5160	54
	1	THF	[(Ph ₃ P) ₃ RhCl] (10 ⁻³)	1380	360
H ₃ Si(CH ₂) ₂ —  —(CH ₂) ₂ SiH ₃	0.5	THF	Bu ₄ NF (10 ⁻³)	35	362
	1	THF	Bu ₄ NF (10 ⁻³)	25	494
	0.5	THF	[(Ph ₃ P) ₃ RhCl] (10 ⁻³)	30	100
	1	THF	[(Ph ₃ P) ₃ RhCl] (10 ⁻³)	20	518
(MeO) ₃ SiCH ₂ —  —CH ₂ Si(OMe) ₃	0.5	MeOH	Bu ₄ NF (10 ⁻²)	45 ^[d]	< 10
	1	MeOH	Bu ₄ NF (10 ⁻²)	20 ^[d]	< 10
	0.5	THF	Bu ₄ NF (10 ⁻²)	< 1	277
	1	THF	Bu ₄ NF (10 ⁻²)	< 1	12
(MeO) ₃ Si—  —	0.5	MeOH	Bu ₄ NF (10 ⁻²)	7	1018
	1	MeOH	Bu ₄ NF (10 ⁻²)	1	1152 ^[f]
	0.5	THF	Bu ₄ NF (10 ⁻²)	4	766
	1	THF	Bu ₄ NF (10 ⁻²)	1	882

[a] The value in parentheses is the concentration of the catalyst [mol L⁻¹]. [b] Gel time. [c] Specific surface area. When the solid exhibits a specific surface area higher than 10 m² g⁻¹ the porosity is dispersed from micro- (< 20 Å) to mesoporosity (200 Å). [d] Precipitate. [e] At -15 °C. [f] The pore size is between 40 and 80 Å.

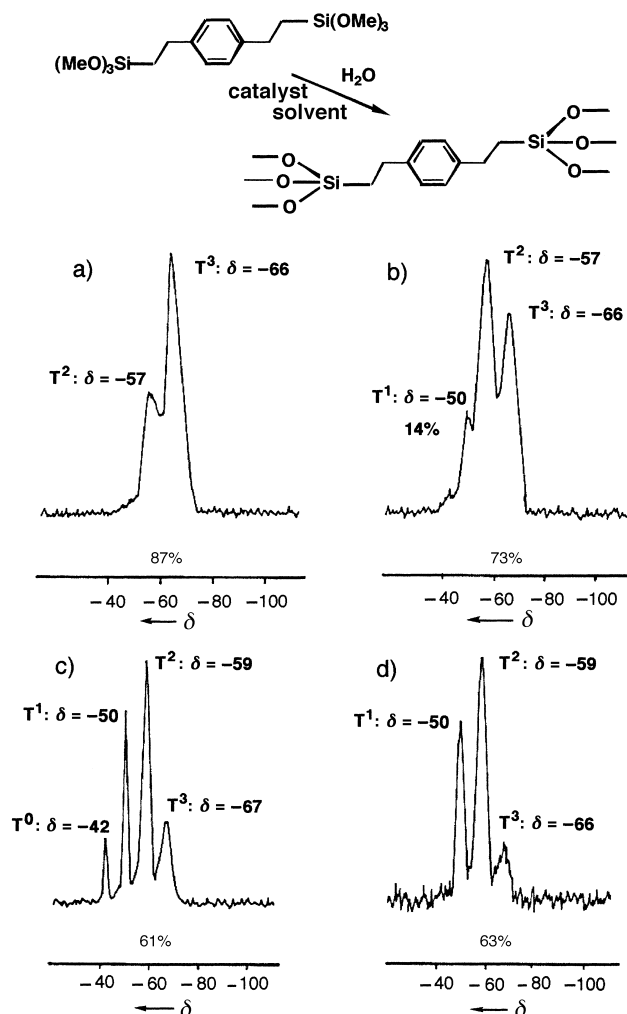
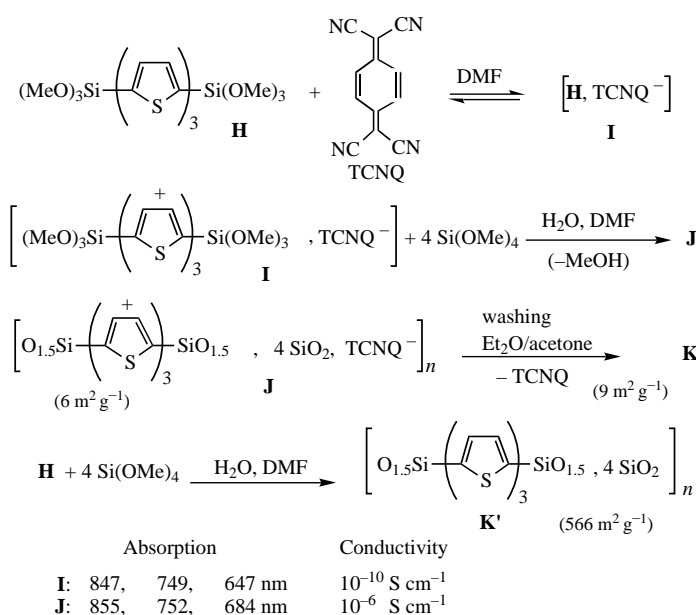


Figure 9. ^{29}Si NMR spectra showing the effect of kinetic parameters on the ratio of polycondensation at silicon: a) THF/ $n\text{Bu}_4\text{F}$; b) THF/ NH_4F ; c) MeOH/ $n\text{Bu}_4\text{F}$; d) MeOH/ NH_4F .



Scheme 19. Effect of the charge-transfer complex [terthiophene · TCNQ] on the formation of the solid.

specific surface ($6 \text{ m}^2 \text{ g}^{-1}$), a visible absorption similar to that of **I**, and a higher conductivity than **I** (10^{-6} instead of 10^{-10} cm^{-1}). The absorption spectrum provides evidence that the charge transfer complex is maintained in the solid. Upon washing with diethyl ether/acetone, a solid (**K**) is obtained and there is a disappearance of both the conductivity and the visible spectrum. This corresponds to destruction of the charge transfer complex.^[23c] This experiment illustrates how weak this interaction is since a simple washing permits its elimination. However, the key point is the comparison of the Brunauer–Emmett–Teller (BET) surface area measured for **J** and **K** (6 and $9 \text{ m}^2 \text{ g}^{-1}$, respectively). A value of $566 \text{ m}^2 \text{ g}^{-1}$ is observed for the solid **K'**, which results from hydrolytic polycondensation performed without TCNQ and under the experimental conditions used for **J**. The two solids **K** and **K'** have the same IR and NMR features, but are very different materials from the point of view of texture.

In conclusion, all these experiments suggest that the formation of the solid is controlled by the kinetics of different chemical steps leading to the solid: polymerization, polycondensation, formation and collapse of colloids. Thus, the texture of the solid might be considered as the result of a very complex kinetic process in which all the experimental parameters play a role. We have checked that the texture can be reproduced by controlling the reaction parameters very carefully. We have observed that it is possible to obtain the same specific surface area and porosity when the experiments are strictly repeated under the same conditions. The preparation must be carried out with the same precision as for physico-chemical experiments. The purity of the solvent (water is a reagent), the purity and concentration of the catalyst and reagents (including water), the temperature, the method of mixing, and the mode of stirring (ultrasonic stirring leads to different textures) are among the factors that could potentially modify the texture. In other words, reproducibility is always possible, but predictability is not. To date, very little is known about the precise mechanisms of polycondensation (initial steps) and aggregation of colloids (gelation). Oxide synthesis by sol–gel processes is considered to lead to unstable solids.^[43] The concept of kinetically controlled solids is more useful since it introduces the possibility of controlling the texture of the solid experimentally by a large number of methods: All the parameters influencing the kinetics of formation listed can be adjusted to control the texture.

7. Short-Range Organization in the Solid

7.1. Generalities

All the nanostructural materials described until now appear as totally amorphous solids since their XRD patterns exhibit signals corresponding to those for amorphous silica. However, XRD patterns are only observed in the case of a solid that exhibits long-range organization. In other words, classical XRD only permits the study of a long-distance organization. Nowadays several methods can be used to probe the “molecular” level (solid-state NMR, X-ray absorption, spectroscopies like XANES and EXAFS). There is no general

physical method that permits study of a short-range organization in solids. Only small-angle X-ray scattering (SAXS) is available for such a purpose; however, until now this technique was used mainly for the macroscopic description of materials.

7.2. Influence of the Molecular Structure on the Solid Organization

In the case of bis-trialkoxysilylated building blocks used for elaboration of nanostructural materials, some preliminary observations have shown that the molecular geometry is a very important parameter in controlling solid organization. Two examples can be given: The first example concerns the results obtained by TOF-SIMS analysis of precursors containing two $\text{Si}(\text{OR})_3$ groups. As reported in Section 5.2 the monosilylated precursors $\text{R}-\text{Si}(\text{OR})_3$ form solids in which the R groups are mainly located at the surface. This was evidenced by TOF-SIMS, which permits detection of mass fragments formed from R .^[60a] With bisilylated systems, the mass fragments corresponding to the organic unit can be detected in only a few cases. Table 5 shows results obtained with three different solids L' , D' , and M' .^[60b]

Table 5. Fragments observed for L' , D' , and M' by TOF-SIMS.

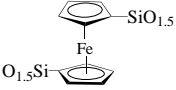
	Xerogel	Ions
L'	$\text{O}_{1.5}\text{Si}-\text{C}_6\text{H}_4-\text{SiO}_{1.5}$	45 (SiOH^+), 59 (SiOCH_3^+)
D'	$\text{O}_{1.5}\text{Si}(\text{CH}_2)_2-\text{C}_6\text{H}_4-(\text{CH}_2)_2\text{SiO}_{1.5}$	77 (C_6H_5^+), 91 (C_7H_7^+)
M'		45 (SiOH^+)

Table 5 illustrates clearly that each case presented here corresponds to a different arrangement of the organic unit in the solid. The TOF-SIMS of L' and M' do not exhibit any fragment corresponding to the molecular units attached to silica, suggesting a solid arrangement in which these moieties are located in the core of the solid. This location can be observed in the case of M' by electrochemistry.^[73] The cyclic voltammogram of M' is characteristic of diffusion-controlled charge transfer: The anodic peak current is linearly proportional to the square root of the scan rate (Figure 10).

The second example is the comparison between L' and D' : Although the two precursors L and D are very similar, the solids L' and D' obtained under the same experimental conditions are completely different. As illustrated in Scheme 20 they behave quite differently.^[64]

Solid L' is hydrophilic and has a high specific surface area ($550 \text{ m}^2 \text{ g}^{-1}$). The SIMS does not exhibit any fragments that derive from C_6H_4 ; only SiOH fragments can be detected. Interestingly, L' does not react with $[\text{Cr}(\text{CO})_6]$, in agreement

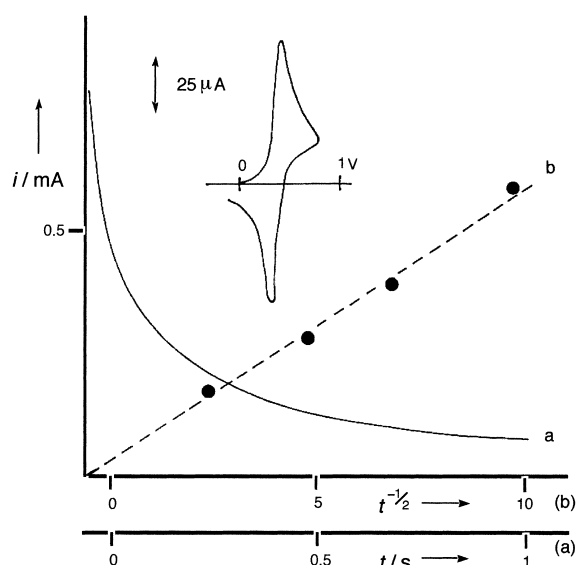
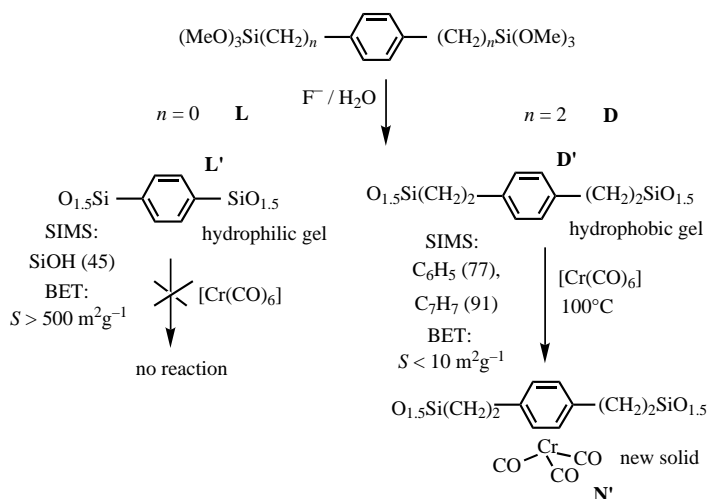


Figure 10. Typical chronoamperometric and linear Cottrell curves of a gel prepared from a bisilylated ferrocene precursor: a) plot of current i versus time t ; b) plot of current i versus $t^{-1/2}$.



Scheme 20. Reactions of gels containing bisilylated phenylene groups.

with the fact that the organic groups are embedded in the core of the solid.

In contrast, D' is a hydrophobic resin with a very poor specific surface area. The TOF-SIMS mass fragments corresponding to the phenyl and benzyl units can be detected; moreover the peak for $\text{Si}-\text{OH}$ peak is not detected.^[60b] These results suggest strongly that the organic groups are located at the surface of the solid. The reactivity of D' is in good agreement with this assumption, since the reaction with $[\text{Cr}(\text{CO})_6]$ takes place with good yield to provide the solid N' (Scheme 20), in which most of the aromatic groups are complexed with $\text{Cr}(\text{CO})_3$ units. This facile complexation is only possible when the aromatic units are accessible.

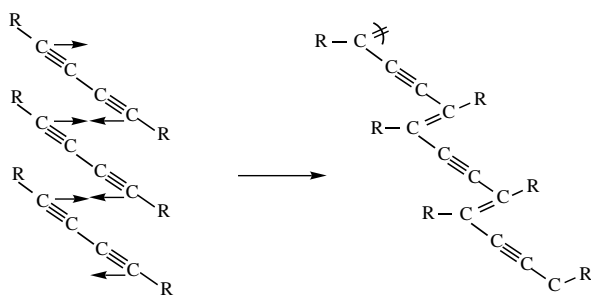
These two examples illustrate very well the importance of the organic unit in controlling the solid arrangement under identical processing conditions. The rigid precursor L leads to a solid L' that is completely different from the solid D' obtained by polycondensation of the more flexible D .

7.3. Chemical Evidence for Short-Range Organization in the Nanostructure

To circumvent the lack of physical methods, the chemical reactivity of the organic component of hybrid solids can provide evidence of short-range organization in amorphous nanostructural materials. The organic moieties can be chosen for selective/specific interactions easily detected spectroscopically and induced by well-defined conditions.

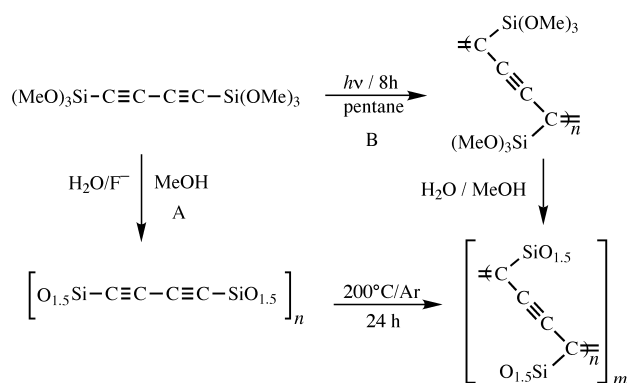
7.3.1. Evidence for Cross-Linking between Diynes Units

As illustrated in Section 3.2, diynes polymerize topochemically by 1,4-addition to form enynes.^[29, 30, 69b] This reaction requires that the C≡C–C≡C units be parallel^[32] (Scheme 21).



Scheme 21. Topochemical polymerization of diacetylene units.

A gel containing diacetylene units was prepared from 1,4-bis(trimethoxysilyl)buta-1,3-diyne (¹³C NMR: $\delta = 79.4, 87.8$ (C≡C–C≡C); IR: $\tilde{\nu} = 2202, 2091 \text{ cm}^{-1}$; Scheme 22). Upon heating at 200 °C under argon, enynes form and the associated



Scheme 22. Synthesis of gels containing bisacetylene units.

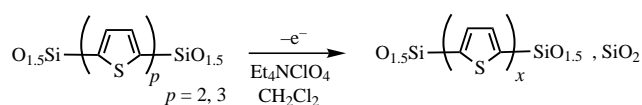
cross-linking is detected by spectroscopy (¹³C NMR: $\delta = 133$; ²⁹Si NMR: $\delta = -74$; IR: $\tilde{\nu} = 2169 \text{ cm}^{-1}$).^[69b] Moreover, the same spectroscopic features result regardless of whether gelation occurs before cross-linking (route A) or whether cross-linking is induced by irradiation before gelation (route B).

One can compare this polymerization with the cross-linking observed for the polymers $[-\text{SiR}_2-\text{C}\equiv\text{C}-\text{C}\equiv\text{C}-]_n$ discussed in Section 3.2. Here, the DTA curve is highly dependent on the organization in the solid.^[29, 30] A sharp peak at 200 °C is observed for the semicrystalline SiMe₂-containing polymer

C1, and a broad peak appears at 350 °C for the amorphous Si(SiMe₃)₂-containing polymer (see Scheme 5). In the case of gels the cross-linking reaction starts at lower temperatures, the DTA exotherm occurs between 100 and 450 °C with a maximum at about 250 °C. The facile reactions between the diyne fragments at relatively low temperatures within the amorphous gel are indicative of a favorable arrangement of the diyne moieties. Enyne formation involves alignment of several diacetylene units within the solid. Since the polycondensation at silicon is mainly T² (C–Si(OSi)₂OR) without any T⁰ (C–Si(OR)₃) observed in the solid, the organic units cannot move in the solid. Thus, these results suggest the presence of short-range order in the nanostructural material, which permits the addition between the organic units.

7.3.2. Polymerization of Thiophene Units in the Solid

Polythiophenes are obtained by electropolymerization,^[79] and silylated thiophenes have been shown to be very efficient precursors, leading to polymers in which the thiophene units are bonded to each other mainly at the α position.^[28a, 80–83] Gels containing bissilylated mono-, bis-, and terthiophene have been prepared. The ¹³C and ²⁹Si CP-MAS NMR spectra show that the structure of the precursor remains intact in the solid without cleavage of the Si–thiophene bond. The electrochemical oxidation of gels deposited as films on electrodes leads to rapid polymerization of the thiophene units in the hybrid matrix^[23c] (Scheme 23).



Scheme 23. Electropolymerization of gels containing silylated thiophenes.

The same reaction is also possible by chemical oxidation using FeCl₃ as the oxidizing agent. The polythiophenes formed in situ by the two methods cannot be separated from the solid; they were identified by Raman resonance spectroscopy ($\tilde{\nu} = 1458, 1220, 1171, 1047, 700, 682, \text{ and } 652 \text{ cm}^{-1}$) and visible absorption.^[23c]

Since polymerization occurs on bissilylated units the polythiophene obtained is terminated by a SiO_{1.5} moiety at each end. This is why it is impossible to separate it from silica, and why it is not possible to characterize the degree of polymerization.

Thus, the fast polymerization occurring in the gel, where the mobility of thiophene units is highly restricted, suggests strongly the presence of short- to medium-range organization within the solid. This conclusion is reinforced when the mechanism of polymerization is taken into account. It is known that oxidative electropolymerization occurs by coupling of two radical cations,^[23c, 82, 83] which has severe stereoelectronic requirements (Figure 11). This coupling involves

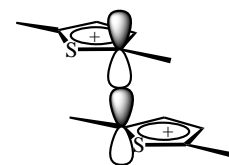


Figure 11. Stereoelectronic requirements for polymerization.

both the close proximity and a parallel arrangement of the two thiophene units.

Thus, the polymerization observed in the cross-linked nanostructural solid suggests strongly the existence of a medium-range organization of thiophene units inside the solid.

8. Control of the Porosity in Silica by Organic Templates

8.1. Generalities

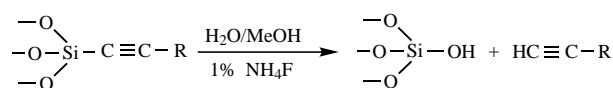
Molecular imprinting is an attractive topic for organic chemistry^[66, 84, 85] since the imprinting of a molecule in a solid can open up interesting possibilities for catalysis and highly selective separations. However, the main difficulties are in finding reliable methods for building up a solid around the molecule (or the group of molecules) without transformation of the geometry and highly selective methods that permit elimination of the molecular unit without any reorganization of the solid network.

Controlling porosity in silica by organic molecular templating is a topic connected to this problem. Many attempts have been made to control the pore size distribution in silica derived by sol-gel techniques.^[86] The general method is to form a hybrid solid by introducing organic templates including micelles, followed by oxidative elimination of the organic component (sacrificial route).^[86-88] The solids used are mostly nanocomposites. However, some nanostructured solids have also been studied, and several narrow pore size distributions have been obtained by these methods.^[84, 85]

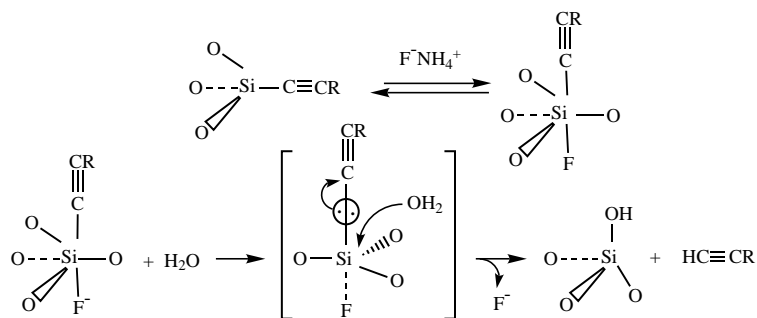
In the course of studies concerning hybrid materials, we sought to develop smooth chemical methods that permitted elimination of the organic unit from a nanostructured material.^[69] The aims of the project were: 1) to find an alternative to the sacrificial route that allows recovery of the organic component under mild conditions; 2) to compare the porosities obtained by oxidation with those obtained by chemical elimination; 3) to consider as building blocks molecular precursors with a rigid and well-defined geometry (linear, planar, or spherical) as well as a very precise size in order to make a more direct comparison between pore size and molecule size; and 4) to compare the porosities obtained from thermal and chemical elimination methods with those occurring from molecular precursors with more flexible organic units.

8.2. Selective Chemical Cleavage

In previous work^[69a] we described methods of cleaving Si-C≡C single bonds under mild conditions using NH₄F as catalyst and H₂O as a reactant (Scheme 24). These catalytic conditions correspond to nucleophilic activation by F⁻ for nucleophilic substitution at silicon. This well-documented process^[91] (Scheme 25) corresponds to reversible coordina-



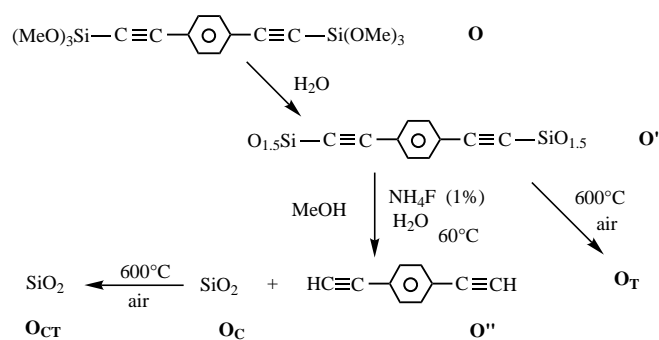
Scheme 24. Catalytic and mild cleavage of Si-C≡C single bonds



Scheme 25. Mechanism of nucleophilic catalysis by F⁻ for cleavage of Si-C≡C single bonds.

tion of F⁻ at silicon, leading to a pentacoordinated center in which the negative charge is delocalized on the substituents bound to silicon. In the second step, nucleophilic attack of H₂O at Si cleaves the Si-C bond with formation of Si-OH and HC≡C-R via a hexacoordinated intermediate.

This selective cleavage was tested with the most simple rigid hybrid (Scheme 26). The precursor **O**, containing two ethynyl groups, generates solid **O'** upon hydrolysis performed without any catalyst. The treatment of **O'** with NH₄F in the presence of H₂O/MeOH at 60 °C results in cleavage of the Si-C bonds and allows almost quantitative recovery of **O''** from **O'** with formation of a templated SiO₂ residue **O_C**.^[84]



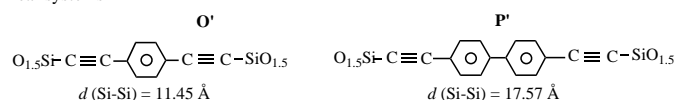
Scheme 26. Selective and quantitative cleavage of the Si-C≡C single bond. **O_T** = SiO₂ solid obtained from precursor **O** after thermal treatment; **O_C** = SiO₂ solid obtained from precursor **O** after chemical treatment; **O_{CT}** = SiO₂ solid obtained from precursor **O** after chemical treatment followed by thermal treatment.

The ¹³C CP-MAS NMR spectrum of **O_C** does not exhibit any signals attributable to **O**. Only signals for the unhydrolyzed OCH₃ groups are observed. After treatment of **O_C** at 600 °C in air, **O_{CT}** is obtained. This silica is carbon-free (less than 0.2%). Another carbon-free silica, **O_T**, can be obtained by thermal treatment (600 °C in air) of the hybrid material **O'**.

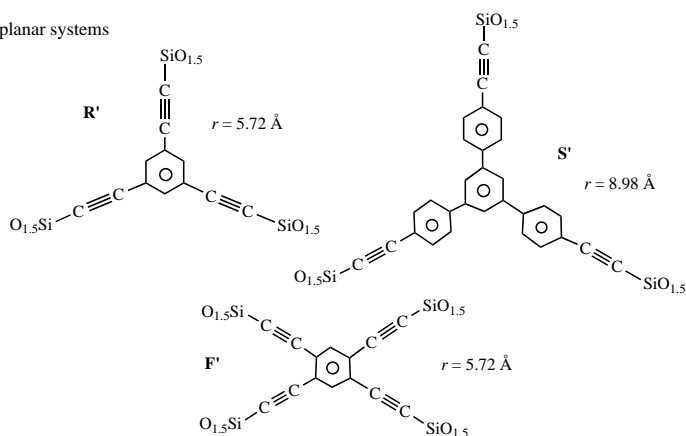
8.3. Studies of Nanostructural Materials

Nanostructural materials obtained using molecular building blocks that have a well-defined size and geometry have been studied and compared to more flexible systems. All the solids were obtained from molecular precursors by hydrolysis without catalysts. They are listed in Scheme 27.^[66]

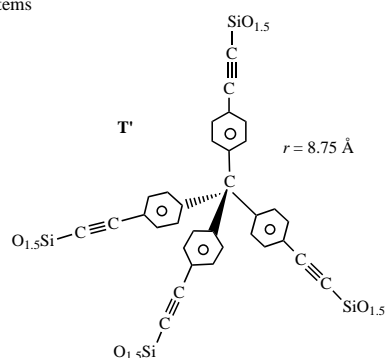
linear systems



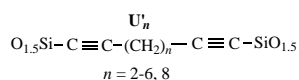
planar systems



globular systems



flexible systems



Scheme 27. Bisacetylenic hybrid materials prepared and treated for elimination of the organic component.

8.4. Results

Scheme 26 shows that depending on the treatment used, **O** provides three kinds of silica: **O_T** (thermal treatment), **O_C** (chemical treatment), and **O_{CT}** (chemical followed by thermal treatment). The same treatment has been carried out on most of the solids listed on Scheme 27.

The first experiments performed were measurements of specific surface areas of the silicas obtained after chemical

treatment. In all cases studied, the elimination of the organic component corresponds to a drastic increase in porosity (Table 6).

Table 6. Specific surface areas *S* of the hybrid materials before treatment and after chemical and thermal treatment.

	<i>S</i> ^[a]	After chemical treatment ^[b]	After thermal treatment ^[c]
O'	19	656	480
R'	45	617	440
S'	25	736	–
T'	717	1090	–
U'₃	< 10	685	–
U'₄	< 10	440	345

[a] Specific surface area (BET) [m² g⁻¹]. [b] NH₄F, H₂O/MeOH, 60 °C. [c] 600 °C in air.

Let us consider now, as an example, the results obtained in the case shown in Scheme 26.^[84] Figure 12 shows the pore size distribution of these materials. Clearly there is a great difference between **O_T** on one hand and **O_C** and **O_{CT}** on the

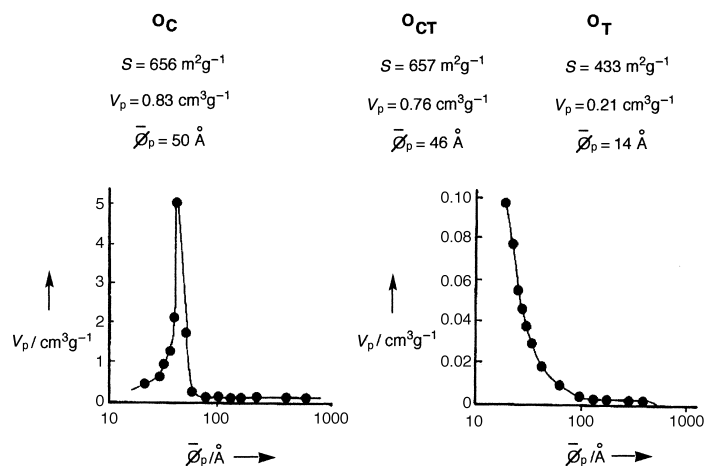


Figure 12. Studies on the textures of silicas obtained from nanostructured hybrid **L**. Comparison of thermal and chemical treatment. *S* = surface area, *V_p* = pore volume, $\bar{\varnothing}_p$ = mean pore diameter.

other. The silica **O_T** exhibits a pore size distribution in the range from about 90 Å to the level of microporosity (< 20 Å). In contrast, **O_C** exhibits a narrow porosity where the maximum is 50 Å. Interestingly both **O_C** and **O_{CT}** (following thermal treatment of **O_C** at 600 °C in air) exhibit almost similar textures (BET, porous volume). The porosity of **O_{CT}** is also narrow (46 Å).

The similarity between **O_C** and **O_{CT}** is supported by SAXS data. This technique permits a direct comparison between the two solids, which exhibit the same diffraction diagram. These data are completely different from that observed for silica obtained by the pyrolytic route (**O_T**; Figure 13), and they are in agreement with the BET results.^[84]

The treatment of the SAXS data^[89] obtained for **O_C** and **O_{CT}** suggests that both silicas follow Porod's law (a slope of *q*⁻⁴ for the linear correlation between ln(*qi*) versus *q*^{2[90]}), corresponding to a clear-cut electronic density between the solid

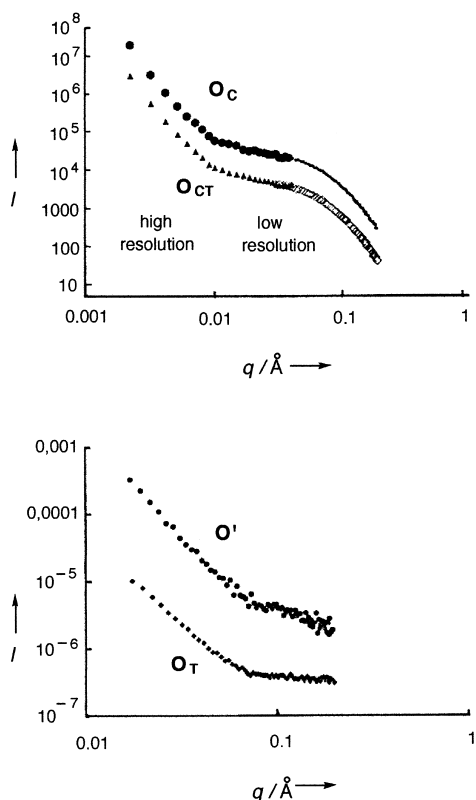


Figure 13. Small-angle X-ray scattering obtained with the solids \mathbf{O}_C , \mathbf{O}_{CT} and \mathbf{O}' ; plots of intensity I versus the scattering vector q , log scale. a.u. = arbitrary units.

silica and the void. This observation is evidence of a smooth surface without roughness and a homogeneous geometry of the pores. Thus the texture of these two silicas may be described as elongated cylinders. A bimodal distribution of pore sizes ((42 ± 2) and (32 ± 2) Å) can be calculated for \mathbf{O}_C and \mathbf{O}_{CT} , respectively. The value of 42 Å can be attributed to porosity by comparison with the BET values (50 Å for \mathbf{O}_C and 46 Å for \mathbf{O}_{CT}). It is not surprising to obtain a different value by SAXS and BET; SAXS focuses on the dominant porosity and the BET provides a measure of the accessible porous volume and is not a direct measure of the pore size. The total value of 32 Å might be assigned to the solid phase surrounded by pores.^[84] The results of transmission microscopy support these conclusions (Figure 14).

As expected, the SAXS data for \mathbf{O}_T exhibits completely different features: A power law of $q^{-3.2}$ is observed, suggesting the possibility of a fractal surface or bushy behavior; that is a surface without regularity and defined geometry.^[84]

The same experiments were performed with the other hybrid solids listed in Scheme 27. Two examples are considered here: In the first instance, the solids are obtained from rigid building blocks having a precise size and geometry (\mathbf{O} to \mathbf{T}). In all cases the results obtained are similar to those described for \mathbf{O} : the BET measurements show that solids obtained after chemical treatment (\mathbf{R}_C) and solids resulting from postthermal treatment (\mathbf{R}_{CT}) exhibit narrow and similar pore size distribution. In contrast, the solids resulting from direct pyrolysis at 600 °C in air (\mathbf{R}_T) show a broad pore size distribution with curves similar to those observed for \mathbf{O} (Table 7).

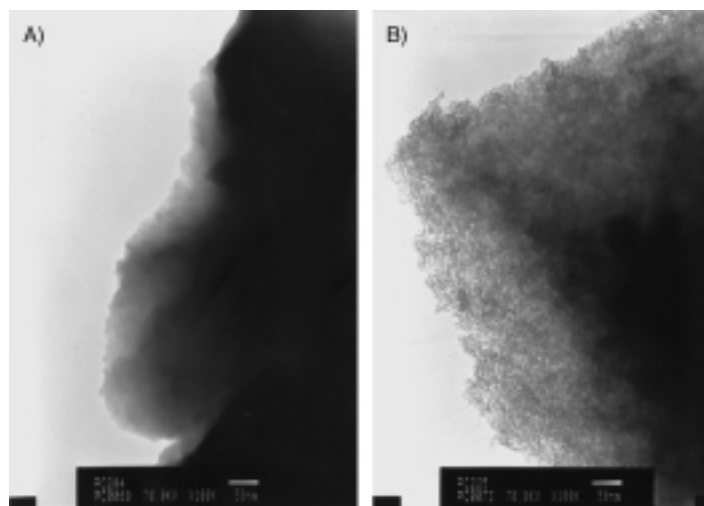


Figure 14. Micrograph of the hybrid material (A) compared to the micrograph of the silica \mathbf{O}_{CT} (B).

Table 7. Specific surface area S and pore volumes V_p of the silicas obtained after chemical and thermal treatment.

Starting material	Silica	S [m ² g ⁻¹]	V_p [cm ³ g ⁻¹]
$\mathbf{O}'(19)$	\mathbf{O}_C ^[a]	656	0.83
	\mathbf{O}_{CT} ^[b]	657	0.76
	\mathbf{O}_T ^[c]	483	0.24
$\mathbf{R}'(45)$	\mathbf{R}_C ^[a]	617	0.68
	\mathbf{R}_{CT} ^[b]	610	0.66
	\mathbf{R}_T ^[c]	440	0.20
$\mathbf{S}'(25)$	\mathbf{O}_C ^[a]	736	1.1
	\mathbf{S}_{CT} ^[b]	706	1.15
	\mathbf{S}_T ^[c]	–	–
$\mathbf{T}'(717)$	\mathbf{P}_C ^[a]	1090	1.05
	\mathbf{T}_{CT} ^[b]	1070	0.9
	\mathbf{T}_T ^[c]	–	–

[a] Chemical treatment. [b] Chemical treatment followed by thermal treatment at 600 °C in air. [c] Direct thermal treatment at 600 °C in air.

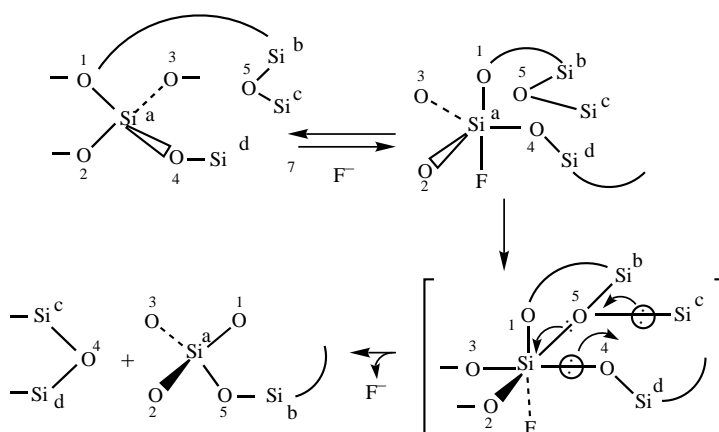
The case of the solid \mathbf{F}' is an exception. As presented in the Section 5.3 cleavage occurs, but the organic molecule cannot be separated from silica.

The silicas obtained from the hybrid solids corresponding to the flexible building blocks $(\text{MeO})_3\text{SiC}\equiv\text{C}(\text{CH}_2)_n\text{C}\equiv\text{C}-\text{Si}(\text{OMe})_3$, \mathbf{U}_n ($n = 2-6, 8$) exhibit completely different behaviors.^[84b, 85] Thermal treatment leads in all cases to the same kind of BET, showing a wide pore size distribution in the range of microporosity (< 15 Å). These curves are similar to those obtained with silicas \mathbf{O}'_1 to \mathbf{T}'_1 resulting from the thermal treatment of hybrid solids \mathbf{O}' to \mathbf{T}' . However, the silicas resulting from chemical treatment, \mathbf{U}_{nC} or \mathbf{U}_{nCT} , do not exhibit a pore size distribution as narrow as those observed for the solids obtained from rigid building blocks. This distribution lies from 27 Å ($n = 2$) to 70 Å ($n = 4$). The SAXS data for \mathbf{U}'_6 after chemical treatment^[85] follow Porod's law with a clear-cut density between the solid silica and the void. Moreover, they show that the geometry of the pores can be described as consisting of elongated cylinders with a diameter of (64 ± 2) Å. This value is in the range of the maximum value measurable by BET (70 Å).

In all cases, the good agreement between BET and SAXS ensures that there are no artifacts in the porosity results. The main observations are as follows:

- 1) In the case of precursors having a well-defined size and rigid geometry, there is a great difference between the narrow porosities observed with chemical elimination versus the wider distribution observed after the sacrificial elimination by oxidation in air.
- 2) It is also interesting to point out the great similarity in the porosity dispersion curves observed after thermal treatment in all cases. All these curves are more or less identical, regardless of the nature of the molecular precursor (rigid or flexible) and its size and geometry. These results and the wider distribution of the pores suggest that thermal treatment cannot be used for molecular imprinting. The silica network does not correlate with the molecular geometry, but is certainly controlled by the thermal rearrangement of SiO_2 .
- 3) The geometry of the precursor is also of importance since only rigid organic components give narrow pore size distributions, regardless of their geometry (linear, planar, or spherical). Flexible structures lead to a wider pore size distribution which exhibits a maximum.
- 4) Although rigid precursors lead to a narrow pore size distribution, there is a large discrepancy between the size of the pores and the size of the organic moiety. The pores obtained are in all cases larger than the molecules used to elaborate the building block.

One possible explanation may be the crossover of two features. The first is the possible short-range organization in the solid occurring during hydrolytic polycondensation of the precursor, which might imply the elimination of more than one organic unit (see Section 7). The second is connected to the reorganization of the solid network during the chemical cleavage of $\text{Si}-\text{C}$ bonds. This chemical reaction catalyzed by NH_4F transforms $\text{R}-\text{SiO}_{1.5}$ into SiO_2 with formation of $\text{Si}-\text{OH}$ bonds (Schemes 24 and 25). This reaction corresponds to an increase in polycondensation at silicon as observed by ^{29}Si NMR spectroscopy.^[66–84a] In competition, the coordination of F^- at silicon can induce a catalytic redistribution of the oxygen atoms around silicon (Scheme 28).



Scheme 28. Reorganization of the silica network catalyzed by F^- .

This redistribution permits complete reorganization of the remaining SiO_2 through formation of new $\text{Si}-\text{O}$ bonds and cleavage of others. As shown in Scheme 28, this process may result in cleavage of chains with formation of rings (or vice versa), inducing the evolution of the solid. Under these circumstances it is not surprising to find pores larger than the size of the molecule.

All these experiments show that the silica is certainly not the best material for molecular imprinting because of its great aptitude to reorganization. However, these results open up interesting perspectives for the rearrangement of silica networks catalyzed by F^- . This rearrangement corresponds to a chemically induced transformation in the texture of a xerogel, occurring by a mechanism which has been established in silicon chemistry. The redistribution induced at silicon by nucleophilic activation is a well-documented process.^[91]

9. Summary and Outlook

This review presents some perspectives on molecular chemistry in the field of material science. The access to SiC is a good illustration of the high flexibility of molecular chemistry. The Yajima process was the first to provide a ceramic with high thermomechanical properties in a rheologically controlled way, leading to films, fibers, or matrices. The adaptability of molecular chemistry has opened further routes to new catalytic processes, new precursors, and even a one-pot procedure.

The combination of molecular chemistry with the wide possibilities opened by the “chimie douce” processes permits access to completely new fields of research in the elaboration of materials. This is based on the very high flexibility of the inorganic polymerization process, which can be easily adapted and combined with organic chemistry. This methodology of materials synthesis is the natural bridge between molecular and solid-state chemistry. The number of possibilities is very large and the field of organic–inorganic materials appears to be a very promising one. It is possible to induce physical and chemical properties with the organic component. Molecular imprinting and chirality in solids are also very exciting open fields. It will be possible to work with matrices other than silica to couple the physical and chemical properties of the organic unit with those of the oxide matrix. In the future, the possibility of working with solids other than oxides will be available by developing polycondensation reactions that permit elaboration of new solid matrices. This chemistry has been already described in the case of nitrides and diimides.^[92]

It is important to point out that kinetic control permits one to play with all the processing parameters and adjust the microstructure of the solid. Moreover, all these hybrid monocomponent materials consist of a homogeneous network. Interestingly, short- to medium-range organization can be observed and presents a challenge to molecular chemists to control the organization of the organic units inside the inorganic network. This control will be the first step in the organization of the physical properties in materials. Owing to the possibility of coupling the chemical and/or physical properties of the organic part and the matrix, it will be

possible to obtain very sophisticated materials. These assertions are not a dream since the chemistry that will permit us to reach these targets exists at the present time.

Finally, this field of research is a great challenge for molecular chemistry because of the very wide possibilities of creating new forms of the matter with expected and unexpected properties. It will be possible to induce the development of a new solid-state chemistry based on kinetic concepts instead of relying on the usual thermodynamic approach. As already pointed out, molecular chemistry, which permits one to investigate these perspectives, is basically known. It simply has to be adapted to the elaboration of mixed solids obtained by polycondensation routes. One of the most illustrative examples given in this review is the access to nanocomposite ceramics, which are accessible only because of the very specific formation of a carbon matrix around the mineral precursor.

I thank my collaborators who have been involved in this chemistry: B. Boury, J. Moreau, M. Enders (SiC); J. Moreau, C. Guerin, B. Henner, W. E. Douglas (conducting polymers); C. Guerin, B. Henner, P. Gerbier (ceramizations from bisalkylenes and nanocomposite ceramics); A. Vioux, D. Leclercq, H. Mutin (sol-gel chemistry); G. Cerveau, J. Moreau, C. Reye, C. Chuit (nanostructured hybrid materials); J. Moreau, M. Wong Chi Man, B. Boury (silicas and geometry of organic template). I also thank all the people who have been working in these field and who are cited in the references. I am grateful to M. Henner for her efficient help in the preparation of this review.

Received: December 8, 1999 [A316]

- [1] R. B. Woodward, *Pure Appl. Chem.* **1973**, 33, 145, and references therein.
- [2] Y. Kishi, *Pure Appl. Chem.* **1989**, 61, 313, and references therein.
- [3] Y. Nagai, H. Matsumoto (Mitsui Toatsu Chemicals Inc.), EP-B 294182, **1989** [*Chem. Abstr.* **1989**, 111, 115975].
- [4] N. Wiberg, C. M. M. Finger, K. Polborn, *Angew. Chem.* **1993**, 105, 1140; *Angew. Chem. Int. Ed. Engl.* **1993**, 32, 1054.
- [5] a) H. G. von Schnering, W. Hönle, *Chem. Rev.* **1988**, 88, 243; b) M. Baudler, *Angew. Chem.* **1987**, 99, 429; *Angew. Chem. Int. Ed. Engl.* **1987**, 26, 419.
- [6] a) P. Chini, *Inorg. Chim. Acta. Rev.* **1968**, 2, 31; b) D. Seyferth in *Advances in Organometallic Chemistry, Vol. 14* (Eds.: F. G. A. Stone, R. West), Academic Press, New York, **1976**, p. 97.
- [7] a) *Polyoxometalates; From platonic solids to anti-retroviral activity* (Eds.: M. T. Pope, A. Müller), Kluwer Academic, Dordrecht, **1994**; b) M. T. Pope, A. Müller, *Angew. Chem.* **1991**, 103, 56; *Angew. Chem. Int. Ed. Engl.* **1991**, 30, 34.
- [8] a) J. P. Majoral, A. M. Caminade, *L'Act. Chim.* **1996**, 4, 13; b) D. A. Tomalia, H. D. Durst, *Top. Curr. Chem.* **1993**, 165, 193.
- [9] M. Verbeek, G. Winter, DE-B 2236078 **1974**, [*Chem. Abstr.* **1974**, 81, 50911].
- [10] a) S. Yajima, Y. Hasegawa, J. Hayashi, M. T. Ilmura, *J. Mater. Sci.* **1978**, 13, 2659; b) Y. Hasegawa, M. T. Ilmura, S. Yajima, *J. Mater. Sci.* **1980**, 15, 720; c) S. Yajima, *Am. Ceram. Soc. Bull.* **1983**, 62, 893.
- [11] J. Rouxel, *Chem. Scr.* **1988**, 28, 33.
- [12] L. Livage, *Chem. Scr.* **1988**, 28, 9.
- [13] a) S. Sakka, K. Kamiya, *J. Non-Cryst. Solids* **1980**, 42, 403; a) "Sol-gel Science": C. J. Brinker, G. W. Scherer, *The Physics and Chemistry of Sol-gel Processing*, Academic Press, San Diego, **1990**; c) L. C. Klein, *Annu. Rev. Sci.* **1985**, 227; d) L. L. Hench, J. K. West, *Chem. Rev.* **1990**, 90, 33; e) C. D. Chandler, C. Roger, M. J. Hampden-Smith, *Chem. Rev.* **1993**, 93, 1205; f) J. Livage, M. Henry, C. Sanchez, *Prog. Solid. State Chem.* **1988**, 18, 259; g) R. Corriu, D. Leclercq, *Angew. Chem.* **1996**, 108, 1524; *Angew. Chem. Int. Ed. Engl.* **1996**, 35, 1420.
- [14] a) B. Boury, L. Carpenter, R. Corriu, *Angew. Chem.* **1990**, 102, 818; *Angew. Chem. Int. Ed. Engl.* **1990**, 29, 785; b) B. Boury, L. Carpenter, R. Corriu, P. Mutin, *New. J. Chem.* **1990**, 14, 535; c) B. Boury, R. Corriu, D. Leclercq, P. H. Mutin, J. M. Planeix, A. Vioux, *Organometallics* **1991**, 10, 1457.
- [15] Recent reviews: R. M. Laine, F. Babonneau, *Chem. Mater.* **1995**, 5, 260; M. Birot, J. P. Pillot, J. Dunogues, *Chem. Rev.* **1995**, 95, 1443.
- [16] C. Aitken, J. P. Barry, F. Gauvin, J. F. Harrod, A. Malek, D. Rousseau, *Organometallics* **1989**, 8, 1732; E. Samuel, J. F. Harrod, *J. Am. Chem. Soc.* **1984**, 106, 1859; J. F. Harrod in *Inorganic and Organometallic polymers with special properties* (Ed.: R. M. Laine), Kluwer Academic Publishers, Dordrecht, **1992**, P. 87, and references therein.
- [17] H. J. Wu, L. V. Interrante, *Chem. Mater.* **1989**, 1, 564.
- [18] R. Corriu, D. Leclercq, P. H. Mutin, J. M. Planeix, A. Vioux, *Organometallics* **1993**, 12, 454.
- [19] R. Corriu, S. Huille, J. Moreau, *10th International Symposium on Organosilicon Chemistry* (Poznan, Poland), **1993**.
- [20] B. Boury, R. Corriu, W. E. Douglas, *Chem. Mater.* **1991**, 3, 487.
- [21] R. Corriu, M. Enders, S. Huille, J. Moreau, *Chem. Mater.* **1994**, 6, 15.
- [22] See, for example, a) R. Riedel, *Naturwissenschaften* **1995**, 82, 12; b) R. Riedel, H. J. Kleebe, H. Schönfelder, F. Aldinger, *Nature* **1995**, 374, 526; c) R. Riedel, W. Dressler, *Ceram. Int.* **1996**, 22, 233; d) R. Riedel, A. Kienzle, W. Dressler, L. Ruwisch, J. Bill, F. Aldinger, *Nature* **1996**, 382, 796.
- [23] a) P. Chicart, R. Corriu, J. Moreau, *Chem. Mater.* **1991**, 3, 8; b) "Inorganic and Organometallic Polymers with Special Properties": P. Chicart, R. Corriu, J. Moreau, F. Garnier, A. Yassar, *NATO ASI Ser. Ser. E* **1992**, 206, 179; c) R. Corriu, J. Moreau, P. Thépot, M. Wong Chi Man, C. Chorro, J. P. Lère-Porte, J. L. Sauvajol, *Chem. Mater.* **1994**, 6, 640.
- [24] a) R. Corriu, W. Douglas, Z. X. Yang, *J. Organomet. Chem.* **1991**, 417, C50; b) R. Corriu, W. Douglas, Z. X. Yang, *Eur. Polym. J.* **1993**, 29, 1563; c) R. Corriu, W. Douglas, Z. X. Yang, *J. Organomet. Chem.* **1993**, 455, 69; d) W. Douglas, D. Guy, A. K. Kar, C. Wang, *Chem. Commun.* **1998**, 2125; e) K. Boyer-Elma, F. Carré, R. Corriu, W. Douglas, *Chem. Commun.* **1995**, 725.
- [25] *Handbook of Conducting Polymers, Vol. 1* (Ed.: T. A. Skotheim), Marcel Dekker, New York, **1985**.
- [26] a) J. L. Bréfort, R. Corriu, P. Gerbier, C. Guérin, B. Henner, A. Jean, T. Kühmann, F. Garnier, A. Yassar, *Organometallics* **1992**, 11, 2500; b) R. Corriu, C. Guérin, B. Henner, A. Jean, T. Kühmann, FR-B 26466162, **1990**.
- [27] M. Ishikawa, Y. Hasegawa, T. Hatano, A. Kunai, *Organometallics* **1989**, 8, 2741; T. J. Barton, S. Iajadi-Maghsoudi, Y. Pang, *J. Polym. Sci. Part A* **1990**, 28, 955.
- [28] a) "Silicon-containing Thiophene Oligomers and Polymers": J. L. Sauvajol, J. P. Lère-Porte, J. J. E. Moreau in *Handbook of Organic Conductive Molecules and Polymers, Vol. 2* (Ed.: H. S. Nalwa), Wiley, New York, **1997**, Kap. 14, P. 625; b) "Silicon and Germanium Containing Conductive Polymers": M. Ishikawa, J. Oshita in *Handbook of Organic Conductive Molecules and Polymers, Vol. 2* (Ed.: H. S. Nalwa), Wiley, New York, **1997**, Kap. 15, P. 685.
- [29] R. Corriu, P. Gerbier, C. Guérin, B. Henner, R. Fourcade, *J. Organomet. Chem.* **1993**, 449, 111.
- [30] R. Corriu, P. Gerbier, C. Guerin, B. Henner, A. Jean, H. Mutin, *Organometallics* **1992**, 11, 2507.
- [31] a) K. J. Wynne, R. W. Rice, *Annu. Rev. Mater. Sci.* **1984**, 14, 297; b) D. Seyferth, G. H. Wiseman in *Science of Ceramic Chemical Processing* (Eds.: L. L. Hench, D. R. Ulrich), Wiley, New York, **1986**, P. 354; c) A. Lavedrine, D. Bahloul, P. Goursat, N. Choong Kwet Yive, R. Corriu, D. Leclercq, H. Mutin, A. Vioux, *J. Eur. Ceram. Soc.* **1991**, 8, 221; d) E. Bacqué, J. P. Pillot, M. Birot, J. Dunogues, P. Lapouyade, E. Bouillon, R. Paillet, *Chem. Mater.* **1991**, 3, 348; e) R. Corriu, D. Leclercq, P. H. Mutin, J. M. Planeix, A. Vioux, *Organometallics* **1993**, 12, 454.
- [32] V. Enkelman, *Adv. Polym. Sci.* **1984**, 63, 91 (polydiacetylenes).
- [33] N. S. Choong Kwet Yive, R. Corriu, D. Leclercq, P. H. Mutin, A. Vioux, *Chem. Mater.* **1992**, 4, 126; F. K. Van Dijen, J. Pluimakers, *J.*

- Eur. Ceram. Soc.* **1989**, *5*, 385; G. T. Burns, G. J. Chandra, *J. Am. Chem. Soc.* **1989**, *72*, 333.
- [34] a) R. Corriu, P. Gerbier, C. Guérin, B. Henner, *Angew. Chem.* **1992**, *104*, 1228; *Angew. Chem. Int. Ed. Engl.* **1992**, *31*, 1195; b) R. Corriu, P. Gerbier, C. Guérin, B. Henner in *Applications of Organometallic Chemistry in the Preparation and Processing of Advanced Materials* (Eds.: J. F. Harrod, R. Laine), Kluwer Academic, Dordrecht, **1995**, P. 203; c) R. Corriu, P. Gerbier, C. Guérin, B. Henner in *Silicon Containing Polymers* (Ed.: R. Jones), The Royal Society of Chemistry, Cambridge, **1995**, P. 3.
- [35] a) E. G. Kendall in *Ceramics for Advanced Technologies* (Eds.: J. E. Hove, W. C. Riley), Wiley, New York, **1965**; b) *Gmelin Handbuch der Anorganische Chemie*, Springer, Heidelberg.
- [36] a) *Transition Metal Carbides and Nitrides* (Ed.: L. E. Toth), Academic Press, New York, **1971**; b) S. Deevi, Z. A. Munir, *J. Mater. Res.* **1990**, *5*, 2177.
- [37] L. M. Berger, *J. Hard Mater.* **1992**, *3*, 3.
- [38] G. V. White, K. J. D. Mackenzie, I. M. Brown, M. E. Browden, J. H. Johnston, *J. Mater. Sci.* **1992**, *27*, 4294.
- [39] R. Corriu, P. Gerbier, C. Guérin, B. Henner, *Adv. Mater.* **1993**, *5*, 380.
- [40] G. Ramis, P. Quintard, M. Cauchetier, G. Busca, V. Lorenzelli, *J. Am. Ceram. Soc.* **1989**, *72*, 1692.
- [41] C. L. Jackson, B. J. Bauer, A. I. Nakatani, J. D. Barnes, *Chem. Mater.* **1996**, *8*, 727.
- [42] a) K. Niihara, *J. Ceram. Soc. Jpn.* **1991**, *91*, 974; b) P. Greil, *J. Eur. Ceram. Soc.* **1998**, *18*, 1905; c) R. T. Paine, J. F. Janik, M. Fan, *Polyhedron* **1994**, *13*, 1225; d) R. T. Paine, C. K. Narula, *Chem. Rev.* **1990**, *90*, 73.
- [43] C. J. Brinker, G. W. Scherer, *Sol-gel Science: The Physics and Chemistry of Sol-gel Processing*, Academic Press, San Diego, **1990**.
- [44] D. C. Bradley, R. C. Mehrotra, D. P. Gaur, *Metal Alkoxides*, Academic Press, New York, **1978**.
- [45] J. Livage, M. Henry, C. Sanchez, *Prog. Solid State Chem.* **1988**, *18*, 259.
- [46] a) R. Corriu, D. Leclercq, A. Vioux, M. Pauthe, J. Phalippou in *Ultrastructure Processing of Advanced Ceramics* (Eds.: J. D. Mackenzie, D. R. Ulrich), Wiley, Chichester, **1988**, P. 113; b) R. K. Iler, *Chemistry of Silica*, Wiley, New York, **1979**.
- [47] a) J. Chojnowski, M. Cypryk, K. Kazmierski, K. Rozga, *J. Non-Cryst. Solids* **1990**, *125*, 40; b) J. Sefcik, A. V. Cormick, *Catal. Today* **1997**, *35*, 205.
- [48] L. P. Hammett, A. J. Deyrup, *J. Am. Chem. Soc.* **1932**, *54*, 2721.
- [49] a) A. Vioux, D. Leclercq, *Heterog. Chem. Rev.* **1996**, *3*, 65; b) A. Vioux, *Chem. Mater.* **1997**, *2292*; d) R. Corriu, D. Leclercq, *Comments Inorg. Chem.* **1997**, *19*, 245.
- [50] a) C. Sanchez, *Mater. Res. Soc. Symp. Proc.* **1994**, *6*; b) C. Sanchez, F. Ribot, *New J. Chem.* **1994**, *18*, 1007 (Sonderheft); c) J. D. Mackenzie, *J. Sol-gel Sci. Technol.* **1994**, *2*, 81; d) J. P. Boilot, F. Chaput, T. Gacoin, L. Malier, M. Canva, A. Brun, Y. Levy, J. P. Galaup, *C. R. Seances Acad. Sci. Ser. 2* **1996**, *322*, 27.
- [51] a) P. Judenstein, C. Sanchez, *J. Mater. Chem.* **1996**, *6*, 54; b) H. K. Schmidt, *Mater. Res. Soc. Symp. Proc.* **1984**, *32*, 327; H. K. Schmidt, *Mater. Res. Soc. Symp. Proc.* **1990**, *180*, 961, and references therein; "Inorganic and Organometallic Polymers": H. K. Schmidt, *ACS Symp. Ser.* **1988**, *360*, 333.
- [52] U. Schubert, N. Hüsing, A. Lorenz, *Chem. Mater.* **1995**, *7*, 2010.
- [53] D. A. Loy, K. J. Shea, *Chem. Rev.* **1995**, *95*, 1431.
- [54] For a general survey, see: a) "Hybrid Organic-inorganic Composites": *ACS Symp. Ser.* **1995**, *585*; b) *New J. Chem.* **1994**, *18* (Special Issue); c) *Tailor-made Silicon Oxygen Compounds, From Molecules to Materials* (Eds.: R. Corriu, P. Jutzi), Vieweg, Braunschweig, **1996**; see also ref. [13g].
- [55] R. Corriu, *Polyhedron* **1998**, *17*, 925; R. Corriu, *C. R. Seances Acad. Sci. Ser. 2* **1998**, *83*; R. Corriu, G. Cerveau, *Coord. Chem. Rev.* **1998**, *180*, 1047; G. Cerveau, C. Chorro, R. Corriu, C. Lepeyre, J. P. Lère-Porte, J. Moreau, P. Thépot, M. Wong Chi Man, *ACS Symp. Ser.* **1995**, *210*; G. Cerveau, P. Chevalier, R. Corriu, C. Lepeyre, J. P. Lère-Porte, J. Moreau, P. Thépot, M. Wong Chi Man, *Tailor-made Silicon Oxygen Compounds, From Molecules to Materials* (Eds.: R. Corriu, P. Jutzi), Vieweg, Braunschweig, **1996**, P. 273.
- [56] P. J. Barri, S. W. Carr, D. Li Ou, A. C. Sullivan, *Chem. Mater.* **1995**, *7*, 265; S. W. Carr, M. Motavelli, D. Li Ou, A. C. Sullivan, *J. Mater. Chem.* **1997**, *7*, 865.
- [57] a) R. Corriu, J. Moreau, M. Wong Chi Man, *J. Sol-gel Sci. Technol.* **1994**, *2*, 87; b) G. Cerveau, R. Corriu, C. Lepeyre, *J. Organomet. Chem.* **1997**, *548*, 99.
- [58] a) C. Eaborn, *Organosilicon Compounds*, Butterworths, London, **1960**; b) L. Birkofer, O. Stuhl in *The Chemistry of Organosilicon Compounds, Part 1* (Eds.: S. Patai, Z. Rappoport), Wiley, New York, **1989**, P. 655.
- [59] a) D. Brunel, *Microporous Mesoporous Mater.* **1999**, *27* (2,3), 329–344; b) D. Brunel, N. Bellocq, P. Sutra, A. Cauvel, M. Lasperas, P. Moreau, F. Di Renzo, A. Galarneau, F. Fajula, *Coord. Chem. Rev.* **1998**, *178–180*, 1085–1108; c) K. Moller, T. Bein, *Chem. Mater.* **1998**, *10*, 2951.
- [60] a) G. Cerveau, J. Dabosi, R. Corriu, J. L. Aubagnac, R. Combarieu, Y. De Puydt, *J. Mater. Chem.* **1998**, *8*, 1761; b) G. Cerveau, R. Corriu, J. Dabosi, C. Lepeyre, R. Combarieu, *Rapid Commun. Mass Spectrom.* **1999**, *13*, 2183.
- [61] V. Belot, R. Corriu, D. Leclercq, P. Lefèvre, P. H. Mutin, A. Vioux, A. M. Flanck in *Chemical Processing of Advanced Materials* (Eds.: L. L. Hench, J. K. West), Wiley, New York, **1992**, P. 143.
- [62] G. Cerveau, C. Lepeyre, *J. Mater. Chem.* **1995**, *5*, 793.
- [63] V. Belot, R. Corriu, D. Leclercq, A. Vioux, M. Pauthe, J. Phalippou, *J. Non-Cryst. Solids* **1990**, *125*, 187.
- [64] G. Cerveau, R. Corriu, C. Lepeyre, *Chem. Mater.* **1997**, *9*, 2561.
- [65] a) K. J. Shea, D. A. Loy, O. W. Webster, *J. Am. Chem. Soc.* **1992**, *114*, 6700; b) M. Mägi, E. Lipmaa, A. Samoson, G. Engelhardt, A. R. Grimmer, *J. Phys. Chem.* **1984**, *88*, 1518; c) G. Engelhardt, H. Jancke, E. Lipmaa, A. Samoson, *J. Organomet. Chem.* **1981**, *210*, 295; d) E. A. Williams in *The Chemistry of Organosilicon Compound, Part 1* (Eds.: S. Patai, Z. Rappoport), Wiley, New York, **1989**, P. 511.
- [66] P. Chevalier, Dissertation, Université Montpellier, **1995**.
- [67] a) K. J. Shea, D. A. Loy, O. W. Webster, *Chem. Mater.* **1989**, *572*; b) K. J. Shea, D. A. Loy, O. Webster, *J. Am. Chem. Soc.* **1992**, *114*, 6700, and references therein; c) K. M. Choi, K. J. Shea, *J. Am. Chem. Soc.* **1994**, *116*, 9052; d) K. M. Choi, K. J. Shea, *J. Phys. Chem.* **1994**, *98*, 3207; e) K. M. Choi, J. C. Hemminger, K. J. Shea, *J. Phys. Chem.* **1995**, *99*, 4720; f) H. W. Oviatt, K. J. Shea, S. Kalluri, Y. Shi, W. H. Steier, L. R. Dalton, *Chem. Mater.* **1995**, *7*, 493; g) D. A. Loy, G. M. Jamison, B. M. Baugher, S. A. Myers, R. A. Assink, K. J. Shea, *Chem. Mater.* **1996**, *8*, 656.
- [68] H. W. Oviatt, Jr., K. J. Shea, J. H. Small, *Chem. Mater.* **1993**, *5*, 943.
- [69] a) R. Corriu, J. Moreau, P. Thépot, M. Wong Chi Man, *Chem. Mater.* **1992**, *4*, 1217; b) R. Corriu, J. Moreau, P. Thépot, M. Wong Chi Man, *Chem. Mater.* **1996**, *8*, 100.
- [70] R. Corriu, J. Moreau, P. Thépot, M. Wong Chi Man, *J. Mater. Chem.* **1994**, *4*, 987.
- [71] G. Dubois, Dissertation, Université Montpellier, **1998**; C. Chuit, R. Corriu, G. Dubois, C. Reyé, unpublished results.
- [72] J. P. Bezombes, C. Chuit, R. Corriu, C. Reyé, *J. Mater. Chem.* **1998**, *8*, 1749.
- [73] a) P. Audebert, P. Calas, G. Cerveau, R. Corriu, N. Costa, *J. Electroanal. Chem.* **1994**, *372*, 275; b) G. Cerveau, R. Corriu, N. Costa, *J. Non-Cryst. Solids* **1993**, *163*, 226.
- [74] R. Corriu, P. Hesemann, G. Lanneau, *Chem. Commun.* **1996**, 1845.
- [75] P. Battioni, E. Cardin, M. Louloudi, B. Schöllhorn, G. A. Spyroulias, D. Mansuy, T. G. Traylor, *Chem. Commun.* **1996**, 2037.
- [76] S. T. Hobson, K. J. Shea, *Chem. Mater.* **1977**, *9*, 616.
- [77] a) G. Cerveau, R. Corriu, C. Fischmeister-Lepeyre, *J. Mater. Chem.* **1999**, *9*, 1149–1154; b) G. Cerveau, R. Corriu, C. Fischmeister-Lepeyre, H. Mutin, *J. Mater. Chem.* **1998**, *8*, 2707–2713; c) G. Cerveau, R. Corriu, E. Framery, *Chem. Commun.*, **1999**, 2081.
- [78] a) S. Hotta, K. Waragai, *Synth. Met.* **1989**, *32*, 395; b) S. Hotta, K. Waragai in *The Physics and Chemistry of Organic Superconductors* (Eds.: G. Saito, S. Kagoshima), Springer, Berlin, **1990**, P. 391.
- [79] a) F. Garnier, *Angew. Chem.* **1989**, *101*, 529; *Angew. Chem. Int. Ed. Engl.* **1989**, *28*, 513; b) F. Roncali, *Chem. Rev.* **1992**, *92*, 711.
- [80] a) M. Lemaire, W. Büchner, R. Garreau, H. Hoa, A. Guy, J. Roncali, *J. Electroanal. Chem.* **1991**, *312*, 547; M. Lemaire, W. Büchner, R. Garreau, H. Hoa, A. Guy, J. Roncali, *J. Electroanal. Chem.* **1990**, *281*,

- 293; b) J. Roncali, A. Guy, M. Lemaire, R. Garreau, H. Hoa, *J. Electroanal. Chem.* **1991**, 312, 277.
- [81] a) P. K. Ritter, R. E. Nofhle, *Chem. Mater.* **1992**, 4, 872; b) H. Matsuda, Y. Taniki, K. Kaeriyama, *J. Polym. Sci. A* **1992**, 30, 1667; c) J. Guay, A. Diaz, R. Wu, J. M. Tour, L. H. Dao, *Chem. Mater.* **1992**, 4, 254.
- [82] J. L. Sauvajol, C. Chorro, J. P. Lère-Porte, R. Corriu, J. Moreau, P. Thépot, M. Wong Chi Man, *Synth. Met.* **1994**, 62, 233.
- [83] M. Bouachrine, J. P. Lère-Porte, J. Moreau, M. Wong Chi Man, *J. Mater. Chem.* **1995**, 5, 797.
- [84] a) P. Chevalier, R. Corriu, P. Delord, J. Moreau, M. Wong Chi Man, *New J. Chem.* **1998**, 423; b) P. Chevalier, R. Corriu, J. Moreau, M. Wong Chi Man, *J. Sol-gel Sci. Technol.* **1997**, 8, 603.
- [85] B. Boury, P. Chevalier, R. Corriu, P. Delord, J. Moreau, M. Wong Chi Man, *Chem. Mater.*, **1999**, 11, 281.
- [86] C. J. Brinker, R. Sehgal, P. L. Hietala, R. Deshpande, D. M. Smith, D. Loy, C. S. Ashley, *J. Membr. Sci.* **1994**, 85.
- [87] N. K. Raman, M. T. Anderson, C. J. Brinker, *Chem. Mater.* **1996**, 8, 1682, and references therein.
- [88] a) C. Roger, M. J. Hampden-Smith, D. W. Schaeffer, G. B. Beaucage, *J. Sol-Gel Sci. Technol.* **1994**, 2, 67, and references therein; b) T. Saegusa, *J. Macromol. Sect. Chem. A* **1991**, 28, 817; c) T. Saegusa, Y. Chujo, *Makromol. Chem. Symp.* **1992**, 64, 1; d) Y. Chujo, H. Matsuki, S. Kure, T. Saegusa, T. Yazawa, *J. Chem. Soc. Chem. Commun.* **1994**, 635; e) C. Roger, M. J. Hampden-Smith, C. Brinker, *J. Mater. Res. Sym. Proc.* **1992**, 271, 51; f) D. A. Loy, R. J. Buss, R. A. Assink, K. J. Shea, H. Oviatt, *Polym. Prepr. Am. Chem. Soc. Div. Polym. Chem.* **1993**, 34, 244.
- [89] a) A. Guinier, *Théorie et Techniques de la Radiocristallographie*, Dunod, Paris, **1956**; b) O. Glatter, O. Kratky, *Small Angle X Ray Scattering*, Academic Press, London, **1982**.
- [90] q is the scattering vector defined by $q = 4\pi \sin \theta / \lambda$ (λ is the wavelength of the X-rays and 2θ the scattering angle).
- [91] a) R. Corriu, C. Guérin, B. Henner, Q. Wang, *Organometallics* **1991**, 10, 3200; b) R. Corriu, G. Dabosi, M. Martineau, *J. Organomet. Chem.* **1978**, 150, 27; R. Corriu, G. Dabosi, M. Martineau, *J. Organomet. Chem.* **1978**, 154, 33; R. Corriu, G. Dabosi, M. Martineau, *J. Organomet. Chem.* **1980**, 186, 25; c) V. Belot, R. Corriu, C. Guérin, B. Henner, D. Leclercq, H. Mutin, A. Vioux, Q. Wang, *Mater. Res. Soc. Symp. Proc.* **1990**, 180, 3, and references therein; d) Ref. [44], and references therein; e) A. Bassindale, P. G. Taylor in *The Chemistry of Organosilicon Compounds, Part 1* (Eds.: S. Patai, Z. Rappoport), Wiley, New York, **1989**, p. 839.
- [92] a) R. Riedel, A. Gabriel, DE-B P1963 4799-8, **1996**; b) A. O. Gabriel, R. Riedel, *Angew. Chem.* **1997**, 109, 371; *Angew. Chem. Int. Ed. Engl.* **1997**, 109, 384; c) D. S. Kim, E. Kroke, R. Riedel, A. O. Gabriel, S. C. Shim, *Appl. Organomet. Chem.* **1999**, 13, 495.